



IEA HPT Annex 52 - Long-term performance monitoring of GSHP systems for commercial, institutional and multi-family buildings

**Case study report for
Forskningen, Stockholm, Sweden**

Three plus energy buildings (by design) with GSHPs, variable-length boreholes, ventilation recovery and pre-heating, wastewater recovery & PV panels

Willem Mazzotti Pallard

November 2021

DOI: [10.23697/dfs2-v474](https://doi.org/10.23697/dfs2-v474)

Preface

This report is part of the work within IEA HPT Annex 52 - *IEA HPT Annex 52 - Long-term performance monitoring of GSHP systems for commercial, institutional and multi-family buildings*, with project period January 1st 2018 to December 31 2021. Annex 52 Operating Agent is Sweden.

Annex 52 aims to survey and create a library of quality long-term measurements of GSHP system performance for commercial, institutional and multi-family buildings. While previous work will be surveyed, the emphasis of the annex is on recent and current measurements. The annex also aims to refine and extend current methodology to better characterize GSHP system performance serving commercial, institutional and multi-family buildings with the full range of features shown on the market, and to provide a set of benchmarks for comparisons of such GSHP systems around the world.

The results from the annex will help building owners, designers and technicians evaluate, compare and optimize GSHP systems. It will also provide useful guidance to manufacturers of instrumentation and GSHP system components, and developers of tools for monitoring, controlling and fault detection/diagnosis. This will lead to energy and cost savings.

The work reported in this document was mainly performed by Willem Mazzotti Pallard at the Royal Institute of Technology (KTH) with support from his colleagues also involved in Annex 52: Alberto Lazzarotto, José Acuña and Mohammad Abuasbeh. Other KTH colleagues, Jonas Anund Vogel, in his quality of director of the KTH Live-in Lab, Safira Figueiredo Monteiro and Davide Rolando, should be thanked for their indirect contributions to the project. In particular, Davide helped building the historical database, which has been useful for this project.

In the text, you will find information and performance analysis of the original testbed of the KTH Live-in Lab: three building on KTH main campus with about 305 student accommodations, 12 boreholes, 3 ground source heat pumps, DHW dominated needs, heat recovery through ventilation and wastewater, 667 PV panels and more. The results specific to these buildings are interesting per say, but there are also more general things discussed, such as data quality and verification – can we blindly trust data? probably not – uncertainty analysis and some design considerations.

The work that has led to this report has been funded by the Swedish Energy Agency (Energimyndigheten) through the project 45979-1.

Summary

The report presents energy system performances for the property *Forskningen* consisting of three modern buildings designed as plus energy houses with 667 PV panels and a heated area of about 10,590 m². The property is located in central Stockholm, Sweden. Special features of the buildings and their shared energy system are

- 11 boreholes of variables lengths (225-350 m) organized in a “flower” configuration with U-pipes
- 1 research borehole (100 m) with coaxial borehole heat exchanger
- heating through energy-recovery ventilation system
- wastewater heat recovery
- Domestic Hot Water (DHW) needs predominant (8 m³ DHW storage)
- desuperheaters used for DHW production
- vapor injection heat pump cycles
- no auxiliary heating system
- apartments well-equipped with sensors (more than 2000 sensors and alarms)
- distributed temperature measurement in boreholes with fiber optics

The monitoring period only extend from 2019-05-26 to 2020-02-03 (except for electricity consumption and production for which data is available for about two years). The energy needs for a full year could nevertheless be estimated and are: 257 MWh/yr (24.3 kWh/(m² yr)) for heating and 442 MWh/yr (41.7 kWh/(m² yr)) for DHW. The ventilation heat recovery (no included in the heating needs) are estimated to cover a large part of the heating supplied to the buildings (about 70%).

Performance factors (PFs) 1, 4, 4+, 5 and 5+ are presented (based on the definitions developed in the Annex 52, see part “Performance metrics” for more details). In addition, two extra PFs are introduced, 5* and 5** which account for the whole fan energy and the ventilation heat recovery, respectively. For the whole monitored period, PF1 is about 3.6 while PF4 and PF5 are about 3.0 and 2.5, respectively.

The electricity values available for about two years allows checking the claim of the buildings being plus energy. Unfortunately, there is a deficit of consumption varying between 50 to 90 MWh/yr.

Besides performances, uncertainties are briefly discussed and the author performs verifications on the available data. It appears that data cannot be blindly trusted and requires a minimum level of interpretation.

A short investigation about the relevance of cooling the ventilation incoming air to recharge the boreholes is conducted and it counter-intuitively appears that it can make sense to do so.

Finally, a list of 10 improvement measures is provided, though some of them perhaps pertain to design considerations and improvements.

Contents

BACKGROUND	4
The buildings	4
The ground source and heat pump systems	7
Monitoring	11
Performance metrics	13
PERFORMANCE MONITORING RESULTS.....	16
Verifications.....	16
Building heating, DHW and cooling loads	20
Ground heat exchanger performance	22
Heat pump performance.....	26
Overall system performance	28
Uncertainty analysis	33
LESSONS LEARNT	36
Design lessons learnt.....	36
High pressure in the brine loop.....	36
Recharging the boreholes through the ventilation.....	37
Performance calculation lessons learnt.....	38
Compressor heat losses and evaporator heat estimation.....	38
Uncertainty related to the sampling frequency.....	39
Data quality and verifications.....	39
Average COP is not the same as SPF.....	39
Improvement measures.....	40
Future work	42
REFERENCES.....	43
Project data access.....	43
Project participants and their contribution	43
APPENDIX	44
Appendix 1 – Component information	44

BACKGROUND

The buildings

The buildings investigated in this report have denomination Forskningsen 2 and are located on the Royal Institute of Technology (KTH) main campus in central Stockholm, Sweden. The three buildings consist of 305 student apartments (rental) and have hosted students since 2017. The three buildings have a total heated area of about 10590 m². Each building is composed of six floors.

The buildings were designed as energy plus buildings. In other words, they are supposed to produce more energy than they consume over a (normal) year (except for individual consumption). The buildings are located in a cold climate and are thus heating dominated. The Domestic Hot Water (DHW) demand represents a large part of the total energy needs of the buildings, perhaps a common feature for modern buildings. Space heating and DHW are provided via Ground Source Heat Pumps (GSHPs). The heat is supplied to the apartments via centralized Air Handling Units (AHUs). The system does not have an auxiliary heating system although heat recovery on wastewater is performed and use to pre-heat DHW. In order to smooth out peak demand from the DHW system, 8 m³ of water tank storage are used. Incoming fresh air to the AHUs can also be pre-heated from the boreholes.



Figure 1. Photos and illustration of the three buildings in Forskningsen 2. Illustration: Semrén & Månsson. Pictures: KTH Live-In Lab.

Cooling is not actively provided although air supplied through ventilation may be conditioned via the borehole heat exchangers¹. The roof is equipped with PV panels as can be seen in Figure 1. A summary of the buildings features is provided in Table 1, while Table 2 includes characteristics of the heat pump system configuration.

Markedly, one of the three buildings host the [KTH Live-In Lab](#), a platform of testbeds enabling “testing of products, services and methods in real buildings”². All three buildings actually are the original testbed(s) of the KTH Live-in Lab and are equipped with a comprehensive set of sensors: indoor CO₂ levels, relative humidity, temperature, electrical meters, etc.

Due to the KTH Live-in Lab, the site has received unusual attention in the media, the construction sector and the research community. As an example, the site was visited by Carl XVI Gustav, King of Sweden.



Figure 2. Location of the Forskningsen 2 site in Sweden

Table 1. Summary of the buildings features

Location	Stockholm, Sweden
Year of building construction	2017
Ground source system operation start date	2017
Building Type	Student apartments
Building floor area (net, gross)	10,590 m ² heated area (>10°C)
Analyzed monitoring start date	2019-05-26 (electricity: 2018-03-20)
Analyzed monitoring period	2020-02-03 (electricity: 2020-06-03)
Unique features of the system	Buildings hosting the KTH Live-in Lab Heating through energy-recovery ventilation system Wastewater heat recovery DHW needs predominant (8 m ³ DHW storage) Desuperheaters used for DHW production Vapor injection heat pump cycles No auxiliary heating system Designed as an energy-plus building (with 667 PV panels) Apartments well-equipped with sensors Distributed temperature measurement in boreholes with fiber optics

¹Each AHU is equipped with a coil heat exchanger allowing for heat exchange between the ground and the incoming air. There are, however, no means of actively cooling the incoming air (e.g. through cooling machines) in the absence of simultaneous heating needs. In other words, the air will be conditioned to the extent that the ground temperature allows for it. More details on that in part “The ground source and heat pump systems”.

²The aim of the KTH Live-in Lab is to accelerate innovation in the building and real-estate sectors by providing a close to real environment in which researchers and companies can test their product or idea.

Table 2. Summary of the system configuration

Heat distribution	Ventilation (32°C / 26°C)
Cooling distribution	Ventilation (no active cooling)
Domestic hot water (DHW) production by system	Heat pumps (same as space heating + desuperheater)
Supplementary heat for space heating	Pre-heating ventilation from boreholes
Supplementary heat for DHW	Wastewater heat recovery for pre-heating
Supplementary cooling	None
Nominal capacity of supplementary heating for space heating	-
Nominal capacity of supplementary heating for DHW	-
Nominal capacity of supplementary cooling	-
Heating load	257 MWh/yr (24.3 kWh/(m ² yr)) ¹
Cooling load	0 MWh/year (0 kWh/m ² ,y)
DHW	442 MWh/yr (41.7 kWh/(m ² yr)) ¹
Heat pump type	Water-to-water
Reversible	No
Compressor type	2 x hermetic inverter scroll with vapor injection
Speeds	Variable speed
Heat pump system	Centralized
Number of heat pumps	3 units
Nominal total heat pump heating capacity	180 kW _{th}
Nominal total heat pump heating capacity available for DHW	180 kW _{th}
Nominal total heat pump cooling capacity	120 kW _{th}
Refrigerant	R410A

¹Normalized to a full year (the monitored period is not a full year)

The ground source and heat pump systems

The ground source system consists of 12 closed-loop boreholes. Of these 12 boreholes, one is used mainly for research and is in general not used by the system. This borehole is 100 m deep and equipped with a coaxial Borehole Heat Exchanger (BHE) consisting of a liner and a PE40 pipe. Pictures of the coaxial BHE under installation are shown in Figure 4. The other boreholes are equipped with more traditional U-pipes heat exchangers (PE40). Except for the 100 m “research borehole”, boreholes are not designed to be vertical as can be seen on Figure 3. Instead, they spread out from the machine room essentially in all directions. Both the actual (measured) and design positions are shown in Figure 3 for each borehole. In addition to being inclined, boreholes also have different lengths. The lengths, inclination and orientation angles for each boreholes are reported in Table 3 (note that there was no borehole 4 in the original nomenclature).

Some of the boreholes are equipped with fiber optics, see the “Monitoring” section for more details.

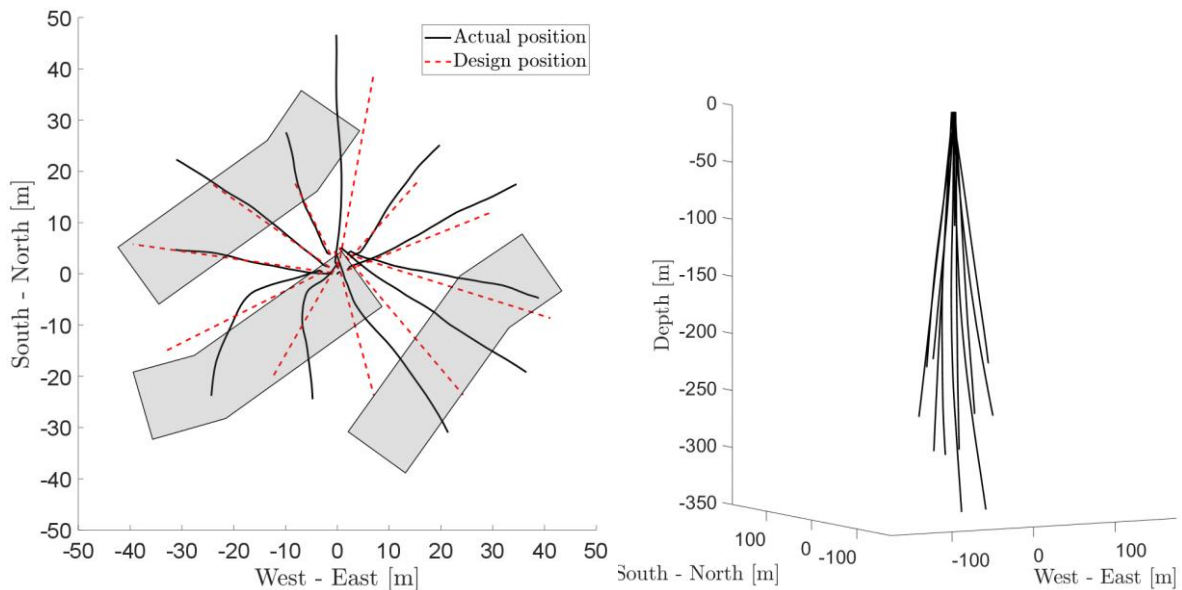


Figure 3. Top view (left) and 3D view (right) of the borehole field in Forsknigen 2

Table 3. Borehole length, inclination and orientation angles

Borehole	Length [m]	Inclination [°]	Orientation [°] ¹
1 (research)	100	0.0	-
2	225	10.0	10
3 ²	225	10.4	105
5	225	10.0	280
6	300	4.0	40
7	270	6.3	70
8	270	7.2	135
9	350	4.0	162
10	350	4.0	212
11	300	6.3	248
12	270	6.3	310
13	300	4.0	340

¹the orientation angle is with North as reference direction (0°) in the clockwise direction

²note that there is no borehole 4 in the original nomenclature



Figure 4. Pictures of the coaxial borehole heat exchanger during installation. Pictures: Patricia Monzó.

A local map of the geological formation (bedrock) is presented in Figure 5. The borehole field is located on a hill and close to metro tunnels, which leads to a relatively low groundwater level: 43 m below the surface. In order to avoid having low, or even negligible, heat transfer between the surface and the groundwater level, all the boreholes are therefore grouted over this section. Only the research borehole is not grouted over this section since the coaxial BHE should allow for somewhat efficient heat transfer within the “dry” section.

The main features of the ground source and BHEs are presented in Table 4 and Table 5, respectively.

The heat pump system consist of three heat pump units, each containing two vapor-compression cycles. The cycles can be qualified as non-conventional since they include a vapor injection line from the condenser outlet to the compressor. The vapor injection limits the discharge temperature at the compressor outlet, which can otherwise be a problem for high-temperature loads such as DHW production. The heat pumps units have reported Seasonal Coefficients Of Performance (SCOPs) of 4.33 and 2.86 under the conditions reported in Table 13 (according to EN 14825). The table also include more ore technical details about the heat pump such as type of heat exchangers and pressure drop characteristics.



Figure 5. Local geological map around the Forsknigen 2 site. Adapted from SGU.

Table 4. Summary of the ground source system

Ground source	Inclined boreholes
Loop type	Closed loop
Ground composition	Metamorphic rocks (see Figure 5)
Groundwater level [m]	43 m
Annual mean air temperature (measured)	8.5 ± 0.7°C (std) ¹ [1], [2]
Undisturbed ground temperature	9.8°C (design 8.0°C)
Design ground thermal conductivity	3.4 W/m,K (assumed)
Volumetric ground heat capacity	2.16 MJ/kg,K (assumed)
Minimum ground heat exchanger exiting fluid temperature (ExFT _{min})	-1.9°C
Maximum ground heat exchanger exiting fluid temperature (ExFT _{max})	18.2°C

¹average and standard deviation for the period 2000-2019.

Table 5. Summary of the ground heat exchanger – Boreholes

Number of boreholes	11+1 (one research borehole)
Borehole length	100 – 350 m
Total borehole length	3085 m + 100 m (research borehole)
Average distance between neighboring boreholes	~10 m
Borehole geometric distribution	“Spider” / “Sunflower” (see Figure 3)
Borehole diameter	115 mm
Borehole filling material	Groundwater and grout (cement)
Borehole heat exchanger type	Single U-tube, Coaxial (research borehole)
Design Effective thermal resistance per unit length	0.05 K·m/W
Source side pipe characteristics	PEM DN40 PN8 (40 mm/35.2 mm)
Source side brine type	Water-Ethanol 28%
Average source side brine flow in operation	7.15 l/s (calculated)

The heat pump system is a centralized system although the distribution is done through air unlike the more common waterborne systems in Sweden. A simplified scheme of the heat pump system is shown in Figure 6. There are eight series-connected water tanks of 1 m³ each on the DHW side and two water tanks of the same volume on the space heating side. The DHW is circulated around the building as is common in Sweden and the cold water is pre-heated with wastewater whenever possible. The circulation pumps on the source side are controlled according to a constant pressure drop setting.

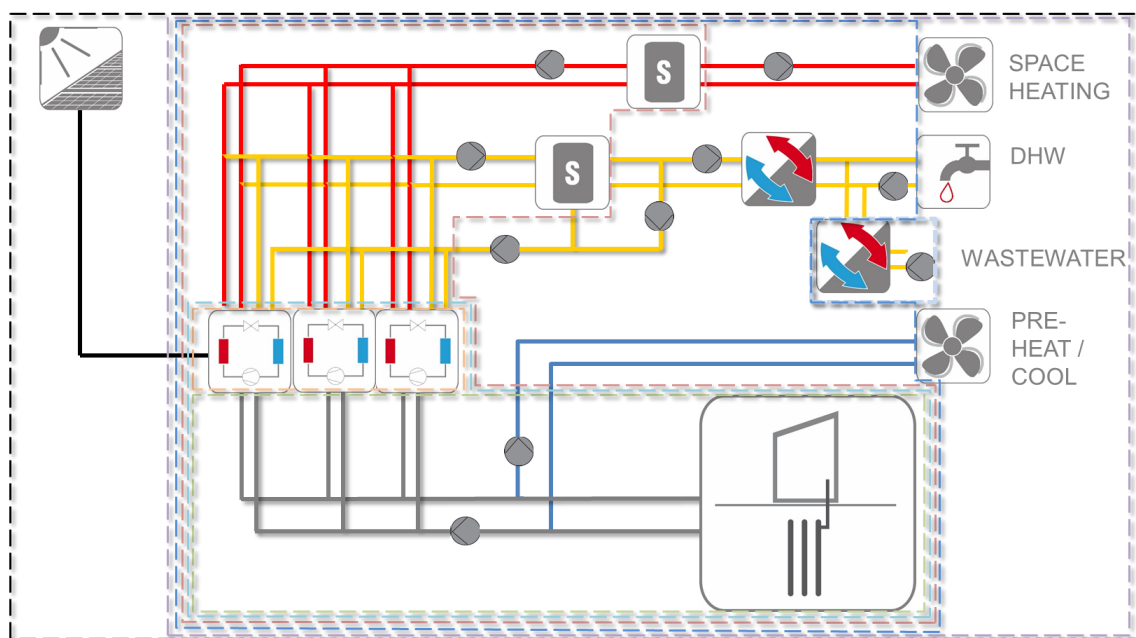


Figure 6. Simplified hydraulic scheme of the central heat pump system. Pictograms by TU Braunschweig IGS, used with permission within the course of IEA HPT Annex 52.

There is a direct connection between the boreholes and AHUs. As shown in the AHU principle scheme in Figure 7, this is done to either pre-heat or cool the incoming air in the AHUs. The AHUs are equipped with two bypasses (not drawn in Figure 7). The first one is a fire fume gas bypass installed between the return and exhaust air. It can also be open when there is no need for heat recovery (e.g. if the exhaust air temperature is warmer than the outdoor air temperature, e.g. due to solar gains) to avoid unnecessary pressure drops through the exhaust filter. The second bypass is installed between the fresh air (after the pre-heating heat exchanger) and supply air. It can be used for controls, for defrosting operation (when water vapor from the return condenses and freezes in the recovery heat exchanger), or summertime.

In addition to the main heating coil shown in Figure 7, there are additional, smaller, heating coils that will adjust the heating level based on the apartments' position and user input, among other things.

A non-exhaustive list of important energy system components are presented in Appendix 1, including product reference, nomenclature name, etc.

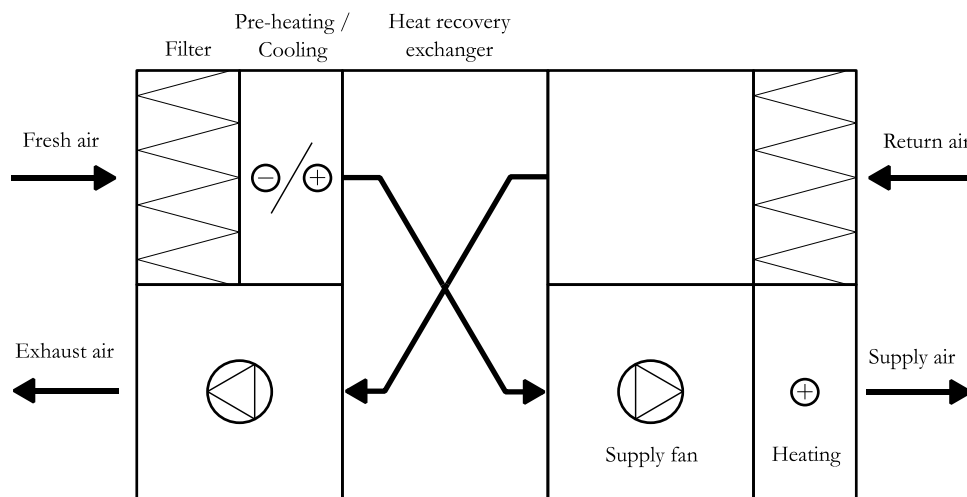


Figure 7. Principle scheme of the AHUs in Forsknigen 2

Monitoring

Since the site is the original testbed of the KTH Live-in Lab, the buildings are equipped with an extensive set of sensors, more than 2000 in total (including alarms and set points). A subset of all sensors of interest for this work are presented in Table 6.

Although data have, in theory, been stored since start of operation (September 2017), different contractual and legal issues have so far prevented researchers from fully accessing all raw data. In particular, most available data are aggregated over hourly intervals and the available period only runs from end of May 2019 to beginning February 2020. Consequently, data and analyses presented in this report are not necessarily representative since they do not cover a full year of operation.

Note, however, that some electrical consumptions are available for more than two years, namely between the end of March 2018 to the beginning of June 2020. Although this is far from giving a complete picture of the buildings energy performance, it is still informative. For instance, the claim of the buildings being plus-energy buildings may be checked.

A special feature of the monitoring system is the fiber optic cables installed in boreholes 1, 3, 6, 10 and 12. Together with a Distributed Temperature Sensing (DTS) equipment, these fiber optic cables allow monitoring the temperature inside the boreholes in a distributed manner along their length. Except for borehole 1, the fiber are installed outside the BHE, that is between the pipe and the borehole wall (in an undetermined location within this space). Unfortunately, the cables in borehole 3 and 6 were buried together with the borehole wellhead under asphalt and are not accessible at the time of writing.

What follows is a brief and largely simplified explanation of how a DTS equipment based on Raman scattering works. A LASER is used to send a single frequency light beam inside the fiber optics. As photons travel through the fiber, they will occasionally collide with the fiber glass molecules. Most of the collisions are elastic, i.e. the photons produced by the collisions will have the same incoming frequency. However, there is a non-zero probability that a shift in frequency, either positive or negative, will occur upon collision. This is referred to as Raman scattering. The probability of occurrence of these shifts is temperature dependent. Thus, temperatures along the length of the fiber can be inferred by measuring these shifts for different times after the initial LASER impulsion.

Another special feature of the monitoring system is that each borehole is equipped with an energy meter (ultrasonic flowmeter and temperature sensors). Unfortunately, though, the data acquisition system does not seem to log any value from any of those meters.

Finally, besides measurement on the centralized energy system, temperature and CO₂ concentration are measured in each of the 300+ apartments. Some apartments are even equipped with some extra sensors.

Table 6. Subset of the system instrumentation of interest for this work

Measurement point	Nomenclature	Instrumentation	Accuracy ¹	
Source side	Boreholes return temperature (outlet)	KB00-GT41	Produal TEAT LL-N	$\pm(0.3 + 0.005 T)$ K
	Boreholes supply temperature (inlet)	KB00-GT42	Produal TEAT LL-N	$\pm(0.3 + 0.005 T)$ K
	Heat pumps supply temperature (inlet)	KB00-GT43	Produal TEAT LL-N	$\pm(0.3 + 0.005 T)$ K
	Heat pumps return temperature (outlet)	KB00-GT44	Produal TEAT LL-N	$\pm(0.3 + 0.005 T)$ K
	AHU supply temperature (inlet)	KB1-GT11	Produal TEAT LL-N	$\pm(0.3 + 0.005 T)$ K
	AHU return temperature (outlet)	KB1-GT41	Produal TEAT LL-N	$\pm(0.3 + 0.005 T)$ K
Heat pumps # = 1,2,3	Heat pump electricity use	VMP#-MQ51 KW	-	-
	Hot gas discharge temperature (circuit 1 or 2)	VMP#-THG41(-42)	-	-
	Inlet evaporator (fluid side)	VMP#-KB SUP. MBV	-	-
	Outlet evaporator (fluid side)	VMP#-KB RET. MBV	-	-
	Inlet condenser (fluid side)	VMP#-VB RET. MBV	-	-
	Outlet condenser (fluid side)	VMP#-VB SUP. MBV	-	-
Load side	Space heating supply temperature (outlet)	VS00-MQ41 GTR	Kamstrup Multical 602	-
	DHW return temperature (condenser)	VS02-MQ41 GTR	Kamstrup Multical 602	-
	DHW return temperature (desuperheater)	VS03-MQ41 GTR	Kamstrup Multical 602	-
	Heat pump condenser supply temperature (outlet)	VS00-GT1#	Produal TEAT LL-N	$\pm(0.3 + 0.005 T)$ K
	Heat pump desuperheater supply temp. (outlet)	VS03-GT1#	Produal TEAT LL-N	$\pm(0.3 + 0.005 T)$ K
	Energy meter space heating	VS00-MQ41	Kamstrup Multical 602	$\pm(0.15 + 2/\Delta T)$ %
	Energy meter DHW condenser	VS02-MQ41	Kamstrup Multical 602	$\pm(0.15 + 2/\Delta T)$ %
Energy meter DHW desuperheater	VS03-MQ41	Kamstrup Multical 602	$\pm(0.15 + 2/\Delta T)$ %	
DHW	Cold water flow rate (total)	KV1-GF41	-	-
	Cold water flow rate to DHW	KV1-GF42	Armatec AT 7420A40	-
	Cold water inlet temperature / after heat recovery	KV1-MQ41	Armatec AT 7274C10	-
	DHW circulation return temperature	VVC1-GT11	Produal TEAT LL-N	$\pm(0.3 + 0.005 T)$ K
	DHW circulation re-heated temperature	VVC1-GT12	Produal TENA LL-N	$\pm(0.3 + 0.005 T)$ K
	DHW supply temperature	VV1-GT11	Produal TENA LL-N	$\pm(0.3 + 0.005 T)$ K
	Energy meter wastewater heat recovery	KV1-MQ41	Armatec AT 7274C10	± 1.5 %
AHU # = 1,...,4	Supply temperature	LB01-GT1	Siemens QAM9020	$\pm(0.3 + 0.005 T)$ K
	Return temperature	LB01-GT2	Siemens QAZ21.5240	$\pm(0.3 + 0.005 T)$ K
	Outdoor temperature	LB01-GT3	Siemens QAZ21.5240	$\pm(0.3 + 0.005 T)$ K
	Exhaust temperature	LB01-GT4	Siemens QAZ21.5240	$\pm(0.3 + 0.005 T)$ K
	Power extraction fan	LB01-FF	-	-
	Power supply fan	LB01-TF	-	-
	Supply air flow rate	LB01-GP1	Siemens QBM69.2512	-
	Extracted air flow rate	LB01-GP2	Siemens QBM69.2512	-
	Supply temperature subsystems 1-8	LB01-GT11(-18)	-	-
Electricity # = 1,2,3	Auxiliary electricity use of the energy plant	EM1-KW	-	-
	Heat pump electricity use	VMP#-MQ51 KW	-	-
	Consumption of the whole energy plant	Bergvärme el	-	-
	Household consumption for the three buildings	Fastighetsel hus#	-	-
	Consumption of the common laundry room	Tvättstuga el	-	-
	Consumption of the fresh water pressurizer	KV-pump el	-	-
	Consumption of the emergency room	Nodrum el	-	-
Bought electricity for each building	Inkommande el hus #	-	-	

¹the accuracy is usually given as a "maximum permissible error" but, unfortunately, without any confidence level. Here we will assume that the errors are uniformly distributed. This distribution is perhaps conservative but we believe that it will also encompass potential accuracy due to onsite installation (e.g. temperature bias due to thermal sensor pockets).

Performance metrics

Even though the electricity consumption of each heat pump is measured directly, only a lumped performance factor for all units can be calculated because only the total heat output is known. Hence, the heat pump performance factor (PF₁) over a given period Δt is computed as

$$PF_1 = \frac{\int_{\Delta t} (\dot{Q}_{desup,DHW} + \dot{Q}_{cond,DHW} + \dot{Q}_{cond,SH}) dt}{\int_{\Delta t} (\dot{W}_{HP1} + \dot{W}_{HP2} + \dot{W}_{HP3}) dt} \quad (1)$$

where the \dot{Q} 's are heat rates, with subscripts referring to the DHW production from the desuperheaters, DHW production from the condensers and the space heating production from the condensers, respectively. \dot{W}_{HPx} is the compressor power for heat pump x .

Unfortunately, the power consumption of the circulation pumps on the source side is not measured and neither is the flow rate. It will be shown later that the flow rates may be estimated but this is still too little information to yield a proper estimation of the pumping energy. Similarly, the power consumption of the circulation pumps between the heat pumps and the storage tanks (DHW or space heating) on the warm side is not known. Hence, neither PF₂ nor PF₃ may be computed with the available data.

The overall energy consumption of the energy plant is however measured, which allows to compute PF₄ as follows

$$PF_4 = \frac{\int_{\Delta t} (\dot{Q}_{HP,tot} + \dot{Q}_{vent,preheating}) dt}{\int_{\Delta t} (\dot{W}_{HP,tot} + \dot{W}_{aux} + \dot{W}_{CW}) dt} \quad (2)$$

where $\dot{Q}_{HP,tot}$ and $\dot{W}_{HP,tot}$ are the total heat rate and power consumption of all three heat pumps, \dot{W}_{aux} is the auxiliary power consumption of the energy plant, \dot{W}_{CW} is the power consumption of the cold water pressurizer (maintaining 4 bar) and $\dot{Q}_{vent,preheating}$ is the amount of air pre-heating through the boreholes. Note that the auxiliary power consumption likely includes external parasitic elements such as external control boards, pressure-lifting pumps and lighting but these are considered negligible in comparison to all the circulation pumps. The wastewater heat recovery may be included in PF₄ as an auxiliary (pre-)heating system such that

$$PF_4^+ = \frac{\int_{\Delta t} (\dot{Q}_{HP,tot} + \dot{Q}_{vent,preheating} + \dot{Q}_{wastewater,DHW}) dt}{\int_{\Delta t} (\dot{W}_{HP,tot} + \dot{W}_{aux} + \dot{W}_{CW}) dt} \quad (3)$$

It should be noted that not all elements between the storage tanks and building distribution are accounted for. In particular, there are three booster circulation pumps – one per building – that is most likely not included in \dot{W}_{aux} . Additionally, the DHW heat taken in eqs.(3)-(4) is the amount of heat charged in the tanks so heat losses that occur in the tank and after are not accounted for. Similarly, heat losses between the space heating tanks and the ventilation are not included.

Now, to get PF₅ one needs simply adding the ventilation energy to the denominator

$$PF_5 = \frac{\int_{\Delta t} (\dot{Q}_{HP,tot} + \dot{Q}_{vent,preheating} + \dot{Q}_{wastewater,DHW}) dt}{\int_{\Delta t} (\dot{W}_{HP,tot} + \dot{W}_{aux} + \dot{W}_{CW} + \dot{W}_{fan,SH}) dt} \quad (4)$$

Note that the ventilation power is integrated only when there space heating is needed in eq.(4). An alternative is to account for the full fan energy regardless of the space heating needs. This alternative performance factor is labelled PF₅^{*}.

The PV cells production, \dot{E}_{PV} , may also be accounted for as an “auxiliary” in PF₅ such that

$$PF_5^+ = \frac{\int_{\Delta t} (\dot{Q}_{HP,tot} + \dot{Q}_{vent,preheating} + \dot{Q}_{wastewater,DHW}) dt}{\int_{\Delta t} (\dot{W}_{HP,tot} + \dot{W}_{aux} + \dot{W}_{CW} + \dot{W}_{fan,SH} - \dot{E}_{PV}) dt} \quad (5)$$

Once again, it should be noted that not all elements of the building distribution system. In addition to the elements previously mentioned, the warm water circulation (VVC) and losses through the ventilation ducts cannot be included. Most of the distribution losses occur within the buildings so they could be considered to space heating to some extent.

The relevance of the PF_5^+ definition may be discussed. For instance, PF_5^+ may become negative if the PV cells production exceed the consumption of the energy systems. Moreover, it is not necessary the case that a large negative value for PF_5^+ is better than a smaller negative value. For instance, overproduction summertime (with respect to the energy systems) will lead to small negative PF_5^+ because the space heating needs are low. Furthermore, there are other elements consuming electricity in the buildings (e.g. lighting) besides the energy systems; PF_5^+ is a poor indicator in that regard. For further discussions about heat pumps and PV cells KPIs, the reader is referred to [3]–[5].

A summary of all performance factors calculated in this study is presented in Table 7. Note that all performance factor definitions are based on the nomenclature developed within Annex 52 – or at least according to its interpretation by the author.

Table 7. Calculated system boundaries for the system according to the Annex 52 boundary schema

Boundary description	HPT Annex 52 Boundary levels				
	H1	H4	H4+	H5	H5+
Ground Source (circulation pumps+ ground source)		X	X	X	X
Heat pump unit including internal energy use, excluding internal circulation pump	X	X	X	X	X
Buffer tank (including circulation pumps between heat pump and buffer tank)		X	X	X	X
Circulation pump on load-side (between buffer tank & building heating distribution system)		X	X	X	X
Building heating distribution system				X	X
Auxiliary (wastewater heat recovery or PV cells)			X		X

There are a couple of time gaps in the data. If the measured values are aggregated (e.g. energy), then the gaps are filled assuming a uniform distribution under the missing period. If the measured values are not aggregated (e.g. flow rate), the gap is arbitrarily filled with an average of prior and posterior values over twice the missing period before and after the gap.

It was previously stated that the flow rates inside the brine loop are not measured. This raises the question of how $\dot{Q}_{vent,preheating}$ is evaluated. Due to lack of temperature and relative humidity data, this power cannot be estimated from the ventilation side. Therefore, the brine flow rate to the ventilation system must be estimated. This can be done in three steps: (1) estimate the evaporators' heat through an energy balance over the heat pump, (2) calculate the brine flow rate over the evaporators through an energy balance and (3) determine the brine ventilation flow rate and the flow rate inside the boreholes through energy balances applied to three different mixing points. The evaporators' heat may be estimated through the following energy balance

$$Q_2 = Q_1 - E_c(1 - \xi) \tag{6}$$

where

- Q_2 is the amount of heat extracted by the heat pumps (evaporator heat)
- Q_1 is the amount of heat supplied by the heat pumps (condenser heat)
- E_c is the electrical energy consumption of the compressors
- ξ is the percentage of heat lost through the compressors' envelope (here ξ is assumed as 5%).

The mass flow rate over the evaporators may then be computed as

$$\dot{m}_{evap} = \frac{\dot{Q}_2}{\Delta T_{evap} \cdot c} \quad (7)$$

where

- ΔT_{evap} is the temperature difference over the evaporators
- c is specific heat capacity of the brine.

The brine thermo-physical properties are here calculated using Coolprop, which itself is based on Melinder's data [6].

Finally, the borehole, heat pump and ventilation brine loops are all interconnected and mixes at three different points (see Figure 29). For each mixing points, an energy balance may be written so that

$$\frac{\dot{m}_{in,1}}{\dot{m}_{out}} = \frac{T_{out} - T_{in,2}}{T_{in,1} - T_{in,2}} \quad (8)$$

with $in, 1$ and $in, 2$ referring to the two mixing branches while out refers to the fluid after mixing. Due to conservation of mass, we also have $\frac{\dot{m}_{in,2}}{\dot{m}_{out}} = 1 - \frac{\dot{m}_{in,1}}{\dot{m}_{out}}$. Using these equations for each of the three mixing points and the heat pump brine mass flow, a system of equation can be solved to estimate the flow rates in the remaining loops.

In that way, the amount of pre-heating may be calculated since the brine supply and return temperature to the ventilation are known. Incidentally, the amount of heat that is recharged in the boreholes through the ventilation can also be computed.

The amount of heat being recovered from the return to the supplied air may however not be properly quantified³. This is due to a lack of information regarding the bypass flows, the air temperature after the pre-heating/cooling coil and the relative humidity (for potential condensation/freezing).

This is also one of reasons for which no cooling PF are presented, in addition to the fact that most cooling happening inside the ventilation system should be regarded as recharging the boreholes rather than comfort cooling. That is, the fresh air may be cooled even at low temperatures, when space heating is required. In such a case, the fresh air first is cooled down by the brine before entering the recovery ventilation heat exchanger and is thereafter is warmed up before being supplied to the building. This poses an immediate question as to the relevance of this setup: why initially cool the air if it needs to be heated eventually? This is discussed in part "LESSONS LEARNT".

For the building heating signature, heat loads are binned with the respect to the outdoor temperature and the heat loads distributions for each bin is presented with the average, the median and the 95% confidence levels. The median is less sensitive to potential outliers which is the reason why it also chosen as indicator.

³ A rough estimation based on the return to exhaust air energy balance is nevertheless made and included in the results section.

PERFORMANCE MONITORING RESULTS

Verifications

In order to ensure that data are of acceptable quality, a couple of verifications is performed. Although it may seem like verifications are not interesting per say, it is the author's conviction that they are an absolute necessity whenever possible. This is to ensure that data is of acceptable quality, that there is no mix up in the sensors and their data storage, that sensors actually measure what they are supposed to, among other things. These verifications may also inform about the measurement uncertainty. Some examples of consistent and inconsistent data are presented in the following paragraphs.

The first verification concerns the evaporator inlet temperature on the fluid side. There at least four different temperature measurements that, in principle, should yield similar results. These are shown in Figure 8, in which heat pump inlet temperatures are plotted vs. the common inlet (VMP1(-2 -3)-KB SUP. MBV vs KB00-GT43). The figure also shows the borehole outlet temperature (KB00-GT41) and the ventilation outlet temperature (KB1-GT41). Data is filtered so as to only show times when all heat pumps are running.

For the different heat pump outlet temperatures, the match is not perfect but within acceptable limits. The evaporator inlet temperatures of heat pump 1, 2 and 3 are in average 0.37, 0.06 and 0.27 K lower than the common inlet temperature. All these differences have standard deviations of about 0.08-0.09 K and seem to be consistent in time. These statistics can be compared with the stated accuracy of about 0.3 K around 0°C.

The borehole and ventilation outlet temperatures do not match but this is expected: there is no reason *a priori* to expect these two temperatures to match. What is expected, however, is that the common heat pump inlet temperature should lie between those two temperatures since the borehole outlet and ventilation outlet streams mix, resulting in the common heat pump inlet. This is observed most of the time but not always, perhaps due to some systematic errors in the measurement or unexpected flow direction.

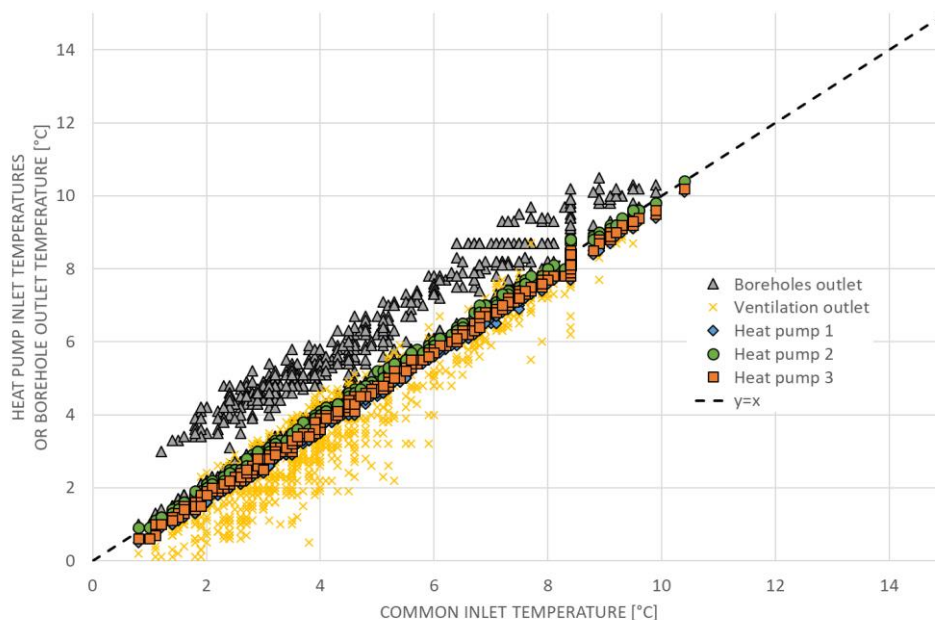


Figure 8. Heat pump evaporator inlet temperatures (fluid side), boreholes outlet temperature and ventilation outlet temperature vs. common inlet temperature (filtered data)

Similarly, in Figure 9 and Figure 10 show other hydraulic mixing points with the mixing temperatures in the vertical axis and the resulting temperature (after mixing) in the horizontal axis. Hence, it is expected that the mixing temperatures are always on each side of the $y = x$ curve. This is what is observed graphically. One of the mixing temperatures may sometimes be equal to the temperature after mixing because of by-pass regulating valves that can be fully closed. Figure 9 shows the stream mixing between the heat pumps common outlet (KB00-GT44) and the borehole outlet (KB00-GT41), which results in the ventilation inlet (KB1-GT11). Figure 10 shows the stream mixing between the heat pumps outlet (KB00-GT44) and the ventilation outlet (KB1-GT41), which result in the borehole inlet (KB00-GT42). It is interesting to notice that the heat pumps common outlet temperature is almost always lower than the borehole and ventilation inlet temperatures (inherently it is also lower than the corresponding outlet temperatures, since those are in general higher than the inlet temperatures during the period of interest). Since the ventilation outlet is higher than the inlet, the air is cooled down before entering the ventilation heat recovery heat exchanger. This has the effect of improving the amount of recovered heat from exhaust air but it unclear if it compensates for the extra load induced by the cooling in itself (see part LESSONS LEARNT for further discussions).

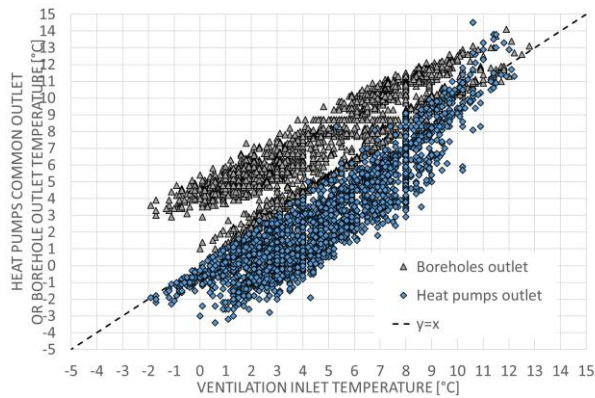


Figure 9. Boreholes and heat pumps outlet temperatures vs. ventilation inlet temperature

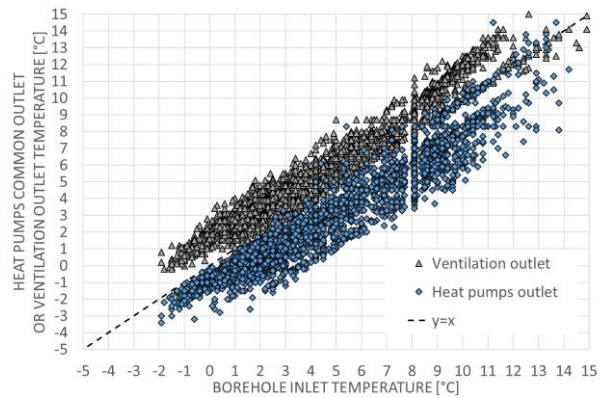


Figure 10. Ventilation and heat pumps outlet temperatures vs. borehole inlet temperature

Similar verifications may be done for the condenser temperatures. Figure 11 shows two different sensors measuring the same thing, namely the outlet condenser temperature of heat pump 1 (fluid side). The data is filtered to show inly times where the heat pump is running.

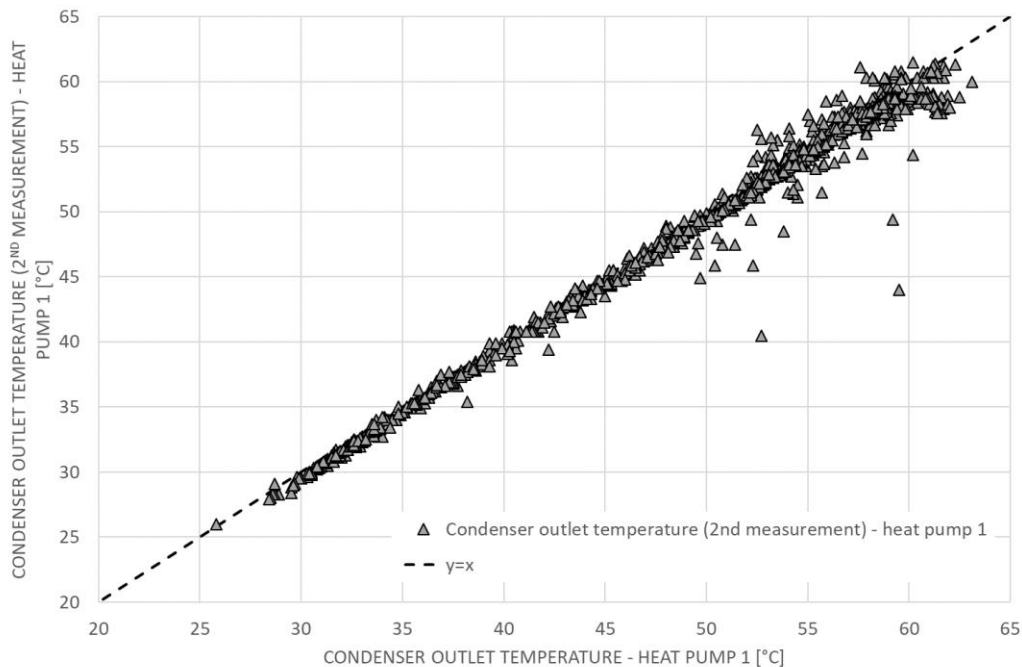


Figure 11. Two different measurements of the condenser outlet temperature of heat pump 1 plotted against each other (filtered data)

The measurements are similar most of the time but there is nevertheless an average difference of about 0.5 K with a standard deviation of 0.76 K. This can be compared with the stated accuracy of about 0.55 K at 50°C (see Table 6). The differences may be due to heat losses, influences from the other heat pumps and/or position of the sensors.

In Figure 12, the monthly energy for DHW production from four different measurement sources is shown. The energy delivered by the heat pumps (from both condenser and desuperheater) and the energy charged in the storage tanks seems to be consistent with one another. However, the energy discharged from the tank is different. If the energy discharged was always lower, heat losses could be a potential explanation but the difference is sometimes positive (e.g. in January 2020) so further investigation is needed to understand this discrepancy.

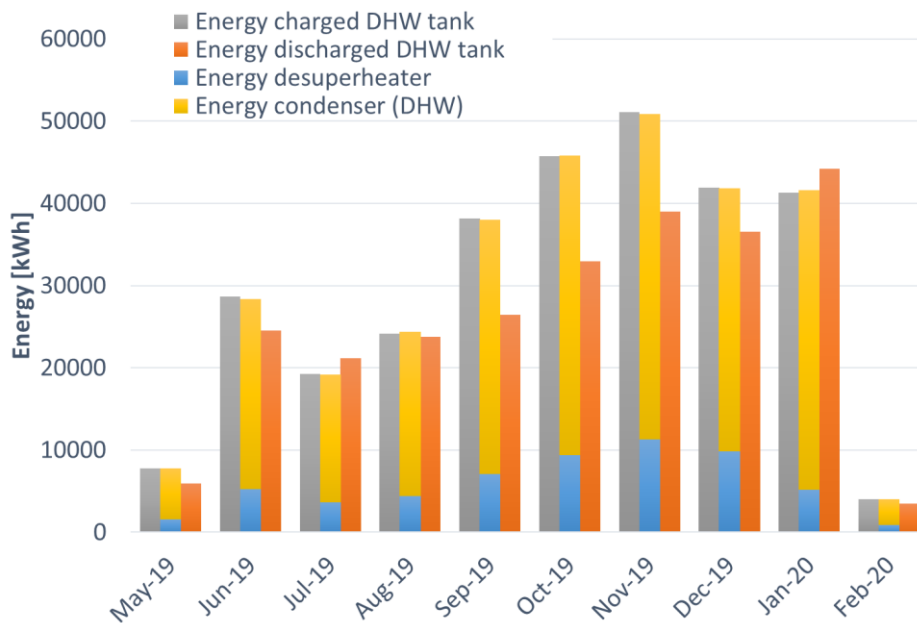


Figure 12. Comparison of monthly DHW energy from three different measurement points

The sensor given the charged and discharged energy is not listed on the hydraulic flowchart, so the position of the latter might be a reason for the observed differences. The values for charged and discharged energy may also be calculated values but the author does not have access to such information. The differences between charged and discharged energy are as high as 25%.

There are two cold water meters, which value could – in theory – be compared to each other. One of them is unfortunately not available (KV1-GF42) but there are several available data from KV1-MQ41 (including KV1-GF41) that can be compared, namely a direct flow measurement, a volume counter and an energy meter (from which the flow rate can be deduced). The three different measurements/estimation are presented in Figure 13.

None of the measurements or estimations match one another. Note that a logarithmic scale is needed to represent all values in the same graph. The direct measurements are too high to be realistic and the two estimated flow rates differ three to ten folds from one another. Here, it is hard to know what data to trust and further investigation is needed to understand these differences. This may affect the values of the wastewater recovery so these should be considered with care when results are presented.

In conclusion, the different “verifications” performed above show that data cannot be blindly trusted and require a minimum level of interpretation. Looking at coarse-grained aggregated data (yearly) may lead to missing some data inconsistencies (e.g. DHW energy).

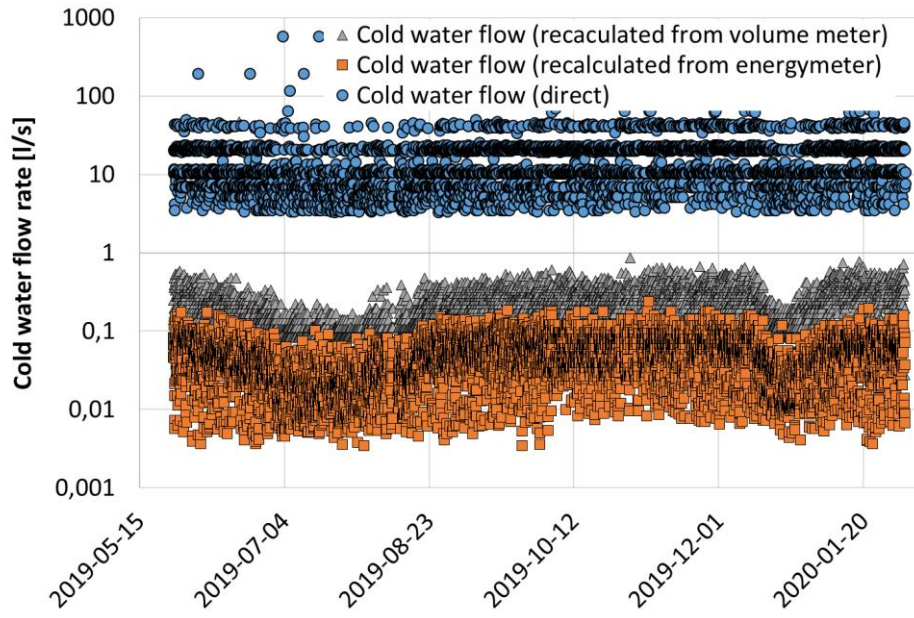


Figure 13. Different values for measured or estimated cold water flow rate

Building heating, DHW and cooling loads

The main characteristics of the building heating and DHW loads are presented in Table 8. Please bear in mind that the values do not represent a whole year of operation and they are not normal-year corrected. The values cannot yet be considered final since the monitoring period does not extend over a full year. DHW appears to be the dominant part of the total loads for the building as can also be observed in Figure 15.

The heating signature of the three buildings are presented in Figure 14 with 95% confidence intervals (2.5th and 97.5th percentiles) and median indicator. The figure includes the heating signature with and without ventilation heat recovery, which is imperfectly estimated based on available data. The relative position of the median and mean may indicate potential outliers. The error bars are quite large, perhaps due to the limited amount of data on which the graph is based but also because the space heating measurement is performed before the storage tanks, which creates some decoupling between outdoor temperature and provided heating.

Table 8. Overall load characteristics

Start of evaluation period	2019-05-26
End of evaluation period	2020-02-03
Building space heating load met by system [MWh _{th}]	177.8
<i>of which ventilation pre-heating [MWh_{th}]</i>	10.9
Building cooling load met by system [MWh _{th}]	-
DHW load met by system [MWh _{th}]	305.7
<i>of which wastewater recovery [MWh_{th}]</i>	3.9
Thermal energy extracted from the ground [MWh _{th}]	247.4
Thermal energy injected to the ground [MWh _{th}]	74.2
Thermal balance ratio (extracted/rejected)	3.3
Heating load (incl. DHW) met by ground source (%)	100
Cooling load met by ground source (%)	100

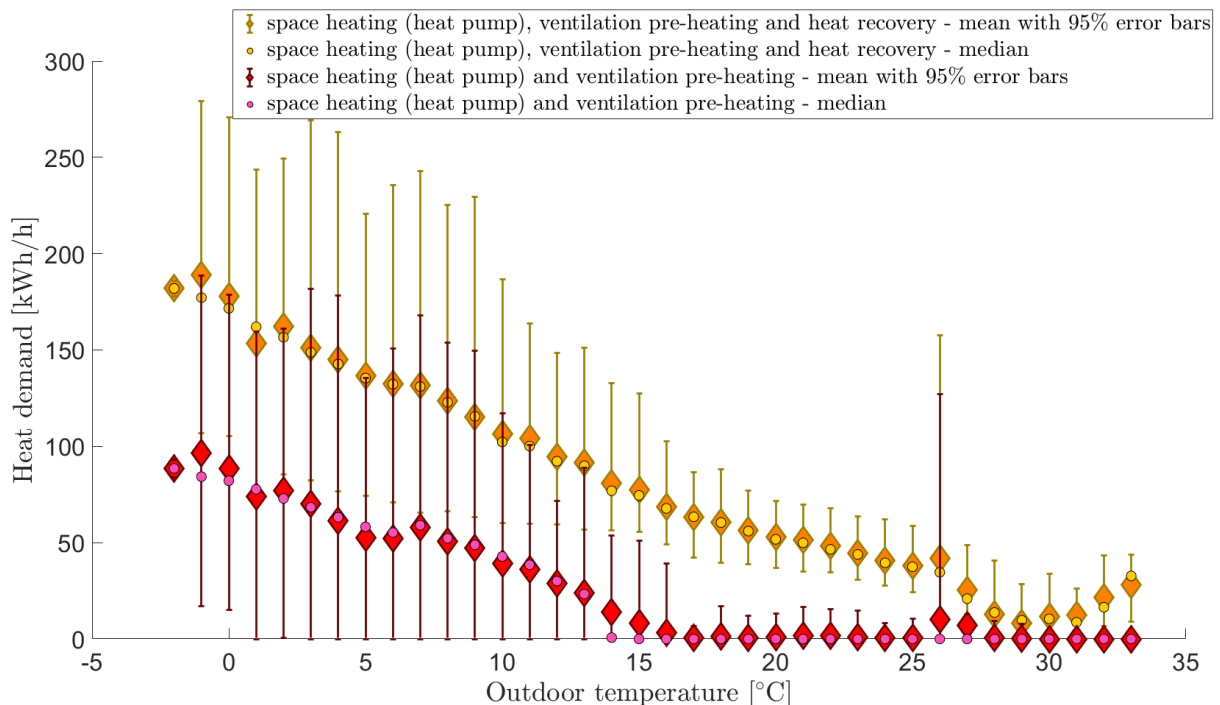


Figure 14. Building energy signatures (heating)

Keeping in mind that the ventilation heat recovery is an estimation, we can nevertheless see that it seems to cover a large part of the building heating needs (about 70%). Note that the energy signature including the ventilation heat recovery is an indication of how the building envelope performs, while the energy signature including only space heating and pre-heating informs about what the energy production system must deliver. The energy signature values including ventilation heat recovery are more uncertain at higher temperatures (regardless of the statistical spread shown in Figure 14), because this is when it is likely that the return air bypass is open towards the exhaust.

Strong assumptions are made in the estimation of the ventilation heat recovery. Namely, that there is no condensation or freezing within the heat exchanger, that the exhaust air bypass is always closed and that there is no heat losses to the ambient.

It should be noted that the space heating needs are not dominant. The DHW needs are instead prevalent. This can be observed in Figure 15 and the trend is believed to be sustained even if a full year operation would have been recorded. For the monitored period, the DHW needs are about 80% higher than the space heating needs.

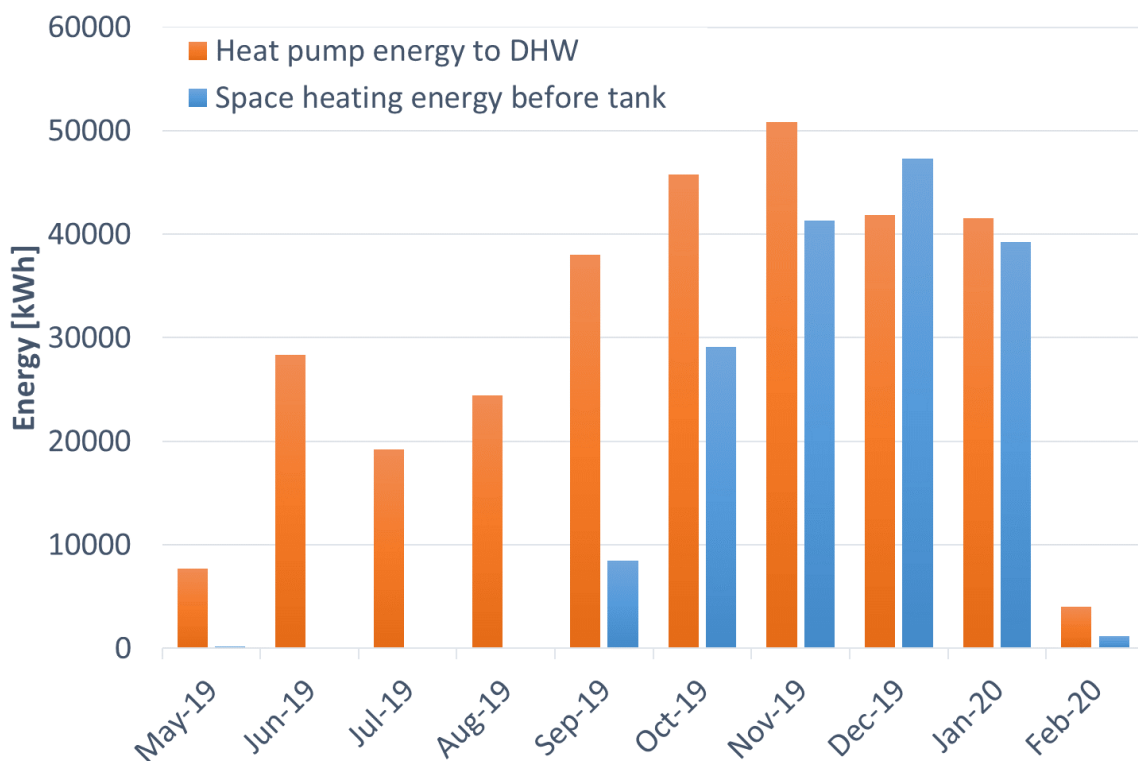


Figure 15. Monthly heating and DHW loads over the monitoring period

Ground heat exchanger performance

The inlet and outlet temperature of the ground heat exchanger between the 26th of May 2019 and the 3rd of February 2020 are presented in Figure 16. The figure also features the daily moving average over the whole period. The lowest temperature reached is -1.9°C while the highest is 18.2°C.

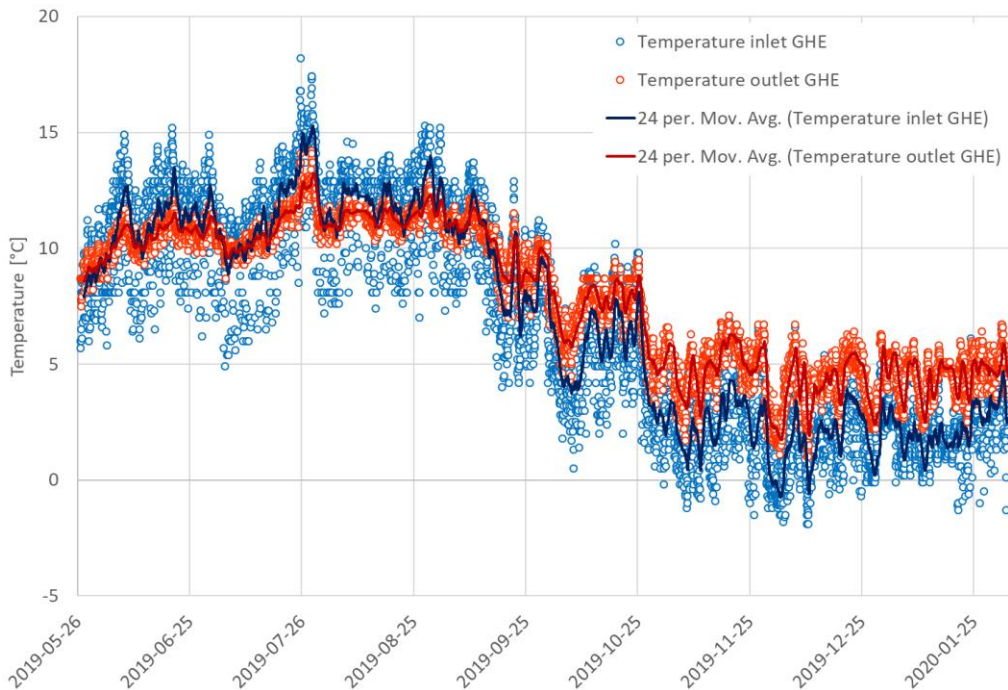


Figure 16. GHE entering and exiting temperatures and their daily moving average over the monitoring period

Based on the temperature profiles summertime, it is likely that some cooling is provided through the Ground Heat Exchanger (GHE). This is indeed what is observed in Figure 17, which shows the energy balance between the heat pump, boreholes and ventilation system. Note that none of the values is directly measured but there seems to be a good match between the energy amounts wintertime. Summertime, differences as high as 28% occur, which reinforce previous statements about the ventilation pre-heating/cooling energy being more uncertain than.

The ventilation energy is always positive, which means that “net-cooling” is provided all year round. Pre-heating also occurs wintertime but it does not show in the monthly aggregation of Figure 17. The term “cooling” may be a bit confusing here, especially wintertime when the outdoor temperature is around 5°C. What is really happening is that the main function of the ventilation pre-heating/cooling coil is to recharge the boreholes – or at least limits the net extracted energy – and not to provide cooling. In principle the fresh air works as an alternative heat source (and it appears so in the aggregation of Figure 17) although the detailed operation shows that it is both recharging the boreholes and being used as heat source directly into the heat pumps.

A last thing that may be noticed is that the boreholes are being recharged (net) summertime.

The total amount of extracted energy from the boreholes is 173 MWh or 56.1 kWh/m of borehole. Note that the 100 m research borehole was not used as part of the GHE during the monitored period. In terms of power, average figures of 21.2 W/m and -12.0 W/m are found for extraction and injection, respectively.

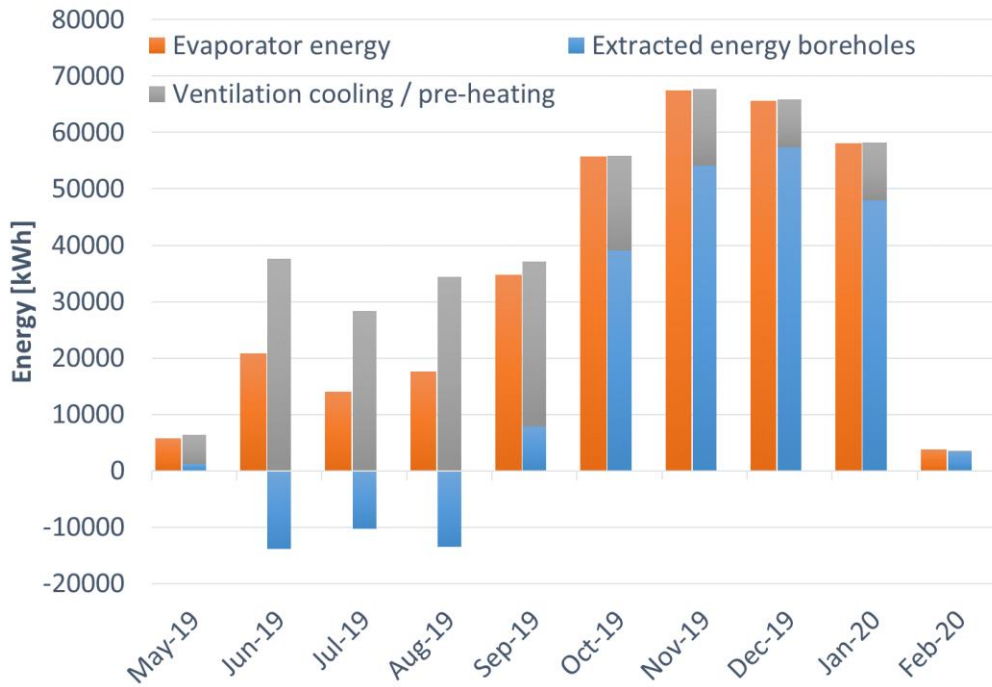


Figure 17. Monthly extracted energy by the heat pumps

The histogram of GHE outlet over the monitoring period is presented in Figure 18 where extraction and injection phase are segregated (note: overlapping histograms). It is clear that the operation mode affects the GHE outlet temperature.

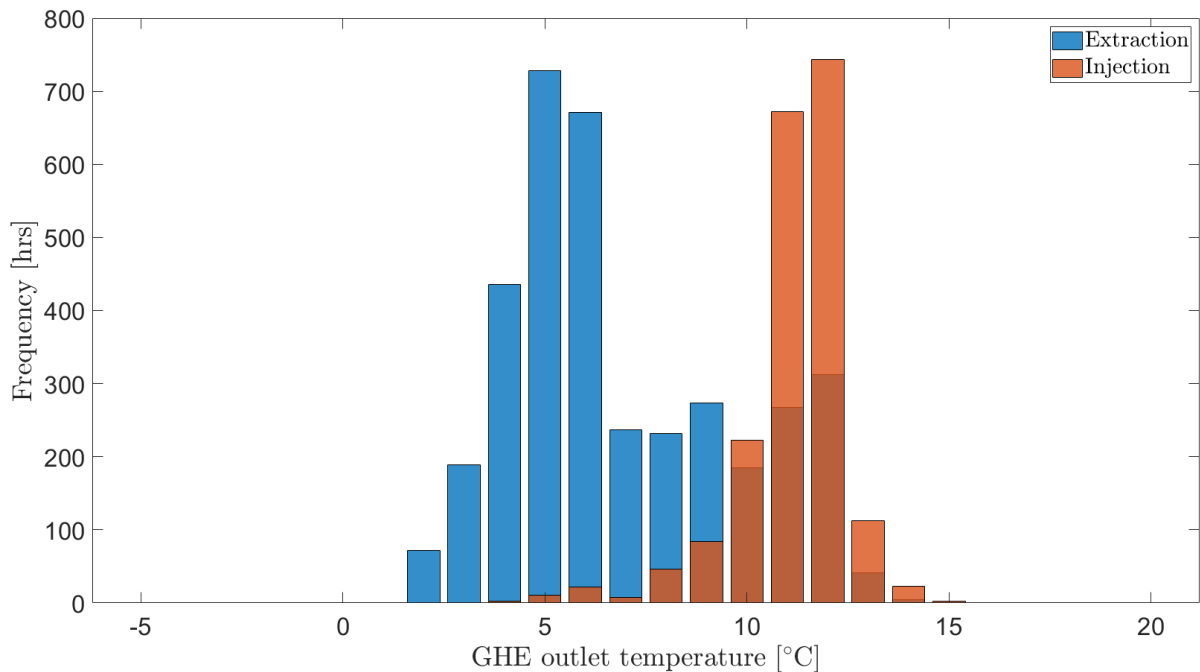


Figure 18. Histograms of GHE outlet temperatures for heat extraction and injection modes

A scatter plot of GHE outlet temperatures vs. outdoor temperatures is displayed in Figure 19. The black dotted line is the $y = x$ line. It is interesting to notice that the GHE outlet is most of time lower than the outdoor temperature, even during periods where heating is needed (e.g. between 5°C and 15°C, see Figure 14). This indicates that Air Source Heat Pumps (ASHP) with the same characteristics of the GSHP would perform better than the GSHPs. However, ASHPs usually have a larger pinch point over the evaporator and the fan might consume more electricity than the GSHP circulation pump. A shifted straight line ($y = x - 3$) is plotted in red in Figure 19 to illustrate the difference in pinch point.

When cooling is potentially needed (about 25°C to 30°C), the GHE temperature is always lower than the outdoor air temperature and sometimes even low enough to provide direct cooling (just circulating in the GHE).

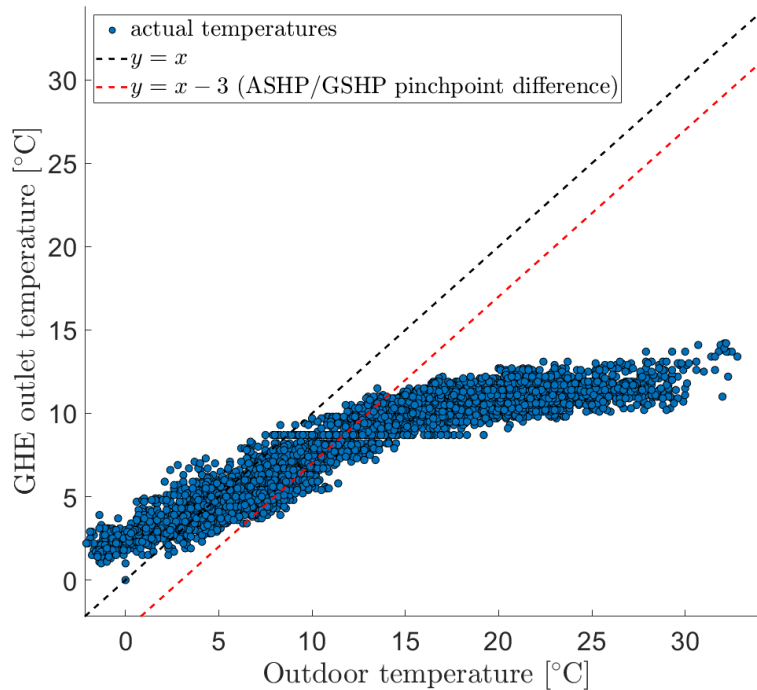


Figure 19. GHE outlet temperature vs outdoor temperature

As previously stated, fiber optic cables are installed in some of the boreholes (between U-pipe and borehole wall). Visualizations of the resulting measurements are shown in Figure 20 and Figure 21 for borehole 10 and 12, respectively. For borehole 10, the temperature profiles for almost a full year, between September 2019 and June 2020 whereas only the autumn period in 2019 is shown for borehole 12. Note the difference in color scale between the two different plots. The presented temperatures are raw and non-calibrated.

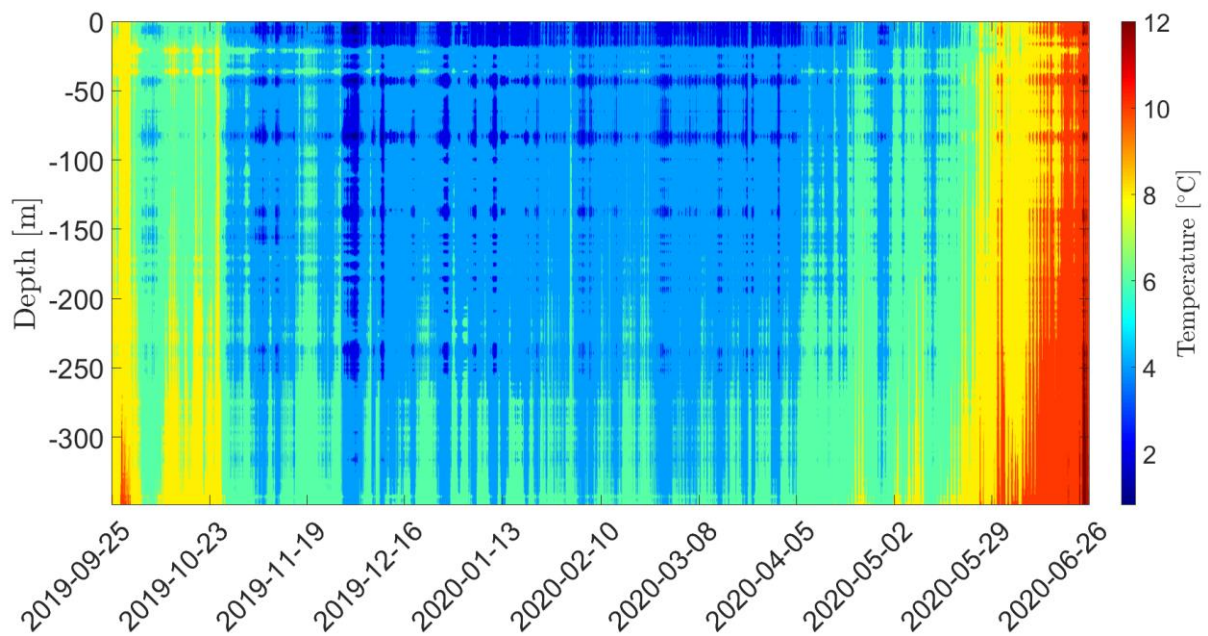


Figure 20. Contour plot of the temperature profile in borehole 10 between September 2019 and June 2020

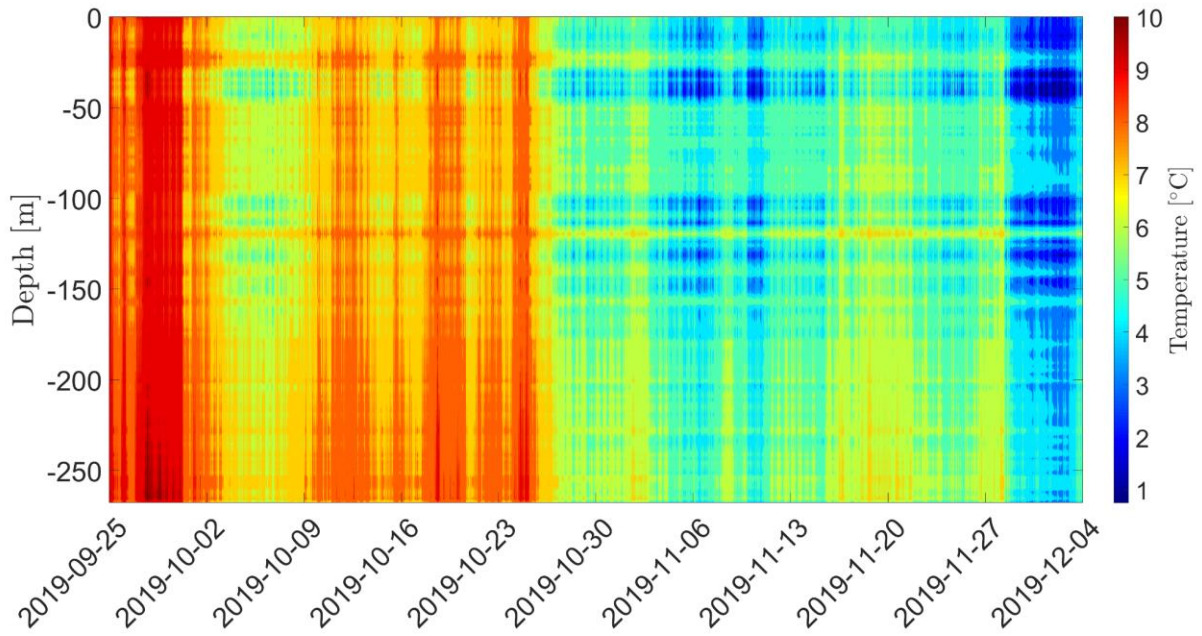
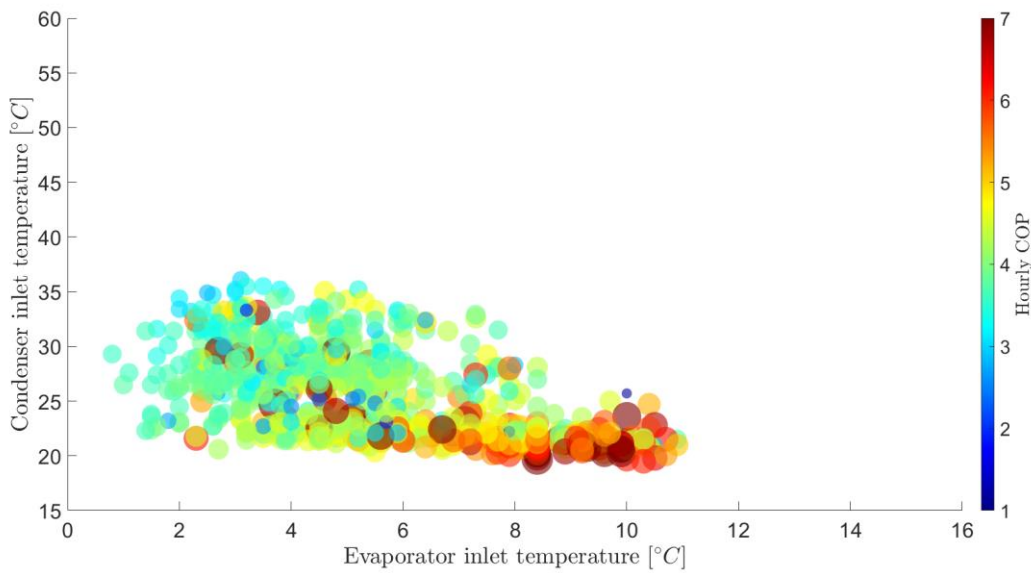


Figure 21. Contour plot of the temperature profile in borehole 12 during autumn 2019

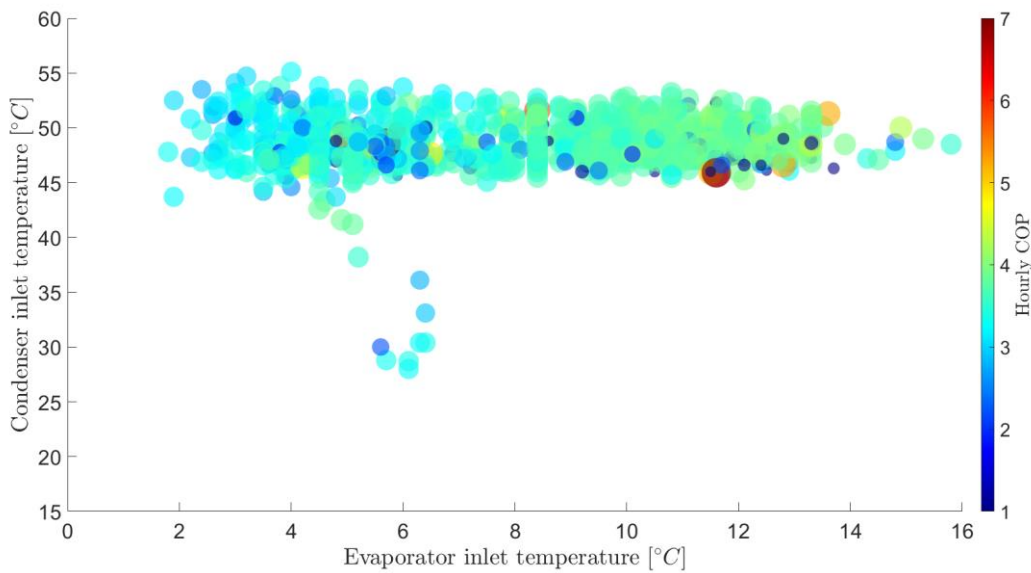
It is interesting to notice that the very top layers of borehole 10 (about 20 meters) are consistently colder even though the borehole is placed under one of the buildings (hence one could expect the top layers to be slightly warmer). On the hand, the boreholes are quite close to each other in these top layers (see Figure 3), which may explain the lower temperatures. Further investigations are needed to clarify this.

Heat pump performance

The hourly COP of the heat pumps during space heating (a) and DHW (b) production is shown in Figure 22. The COPs are color-coded. Note that data were filtered for COP higher than 10 and that only non-simultaneous space heating and DHW productions are shown (filter of 5 kW). Because of the large spread of COP and temperature values, it is perhaps hard to see a clear tendency. One can notice that COPs are in general lower during DHW production due to higher inlet temperatures. For space heating, COPs seem to increase with increasing evaporator inlet temperature as can be expected. The influence of the condenser inlet temperature is however harder to see.



(a). Space heating



(b) Domestic Hot Water

Figure 22. Hourly COP for different evaporator and condenser inlet temperatures (filtered for COP higher than 10)

There are some outliers in Figure 22 (e.g. high COPs) but data presented in both graphs may be used to fit a performance map that may give a clearer indication of how the heat pump performs under different conditions. Here the fitted map is chosen as a quadratic law in both input variables (namely the condenser inlet and evaporator inlet temperatures). There are of course other parameters that influence the heat pump performance (e.g. condenser and evaporator flow rates). The fitted map should not be seen as an exact predictor of the heat pump COP – especially for conditions for which data points are scarce – but rather as an indication of performance. Here, the heat pump performance behaves exactly as expected: higher evaporator inlet temperature and lower condenser inlet temperature lead to higher COPs and vice-versa.

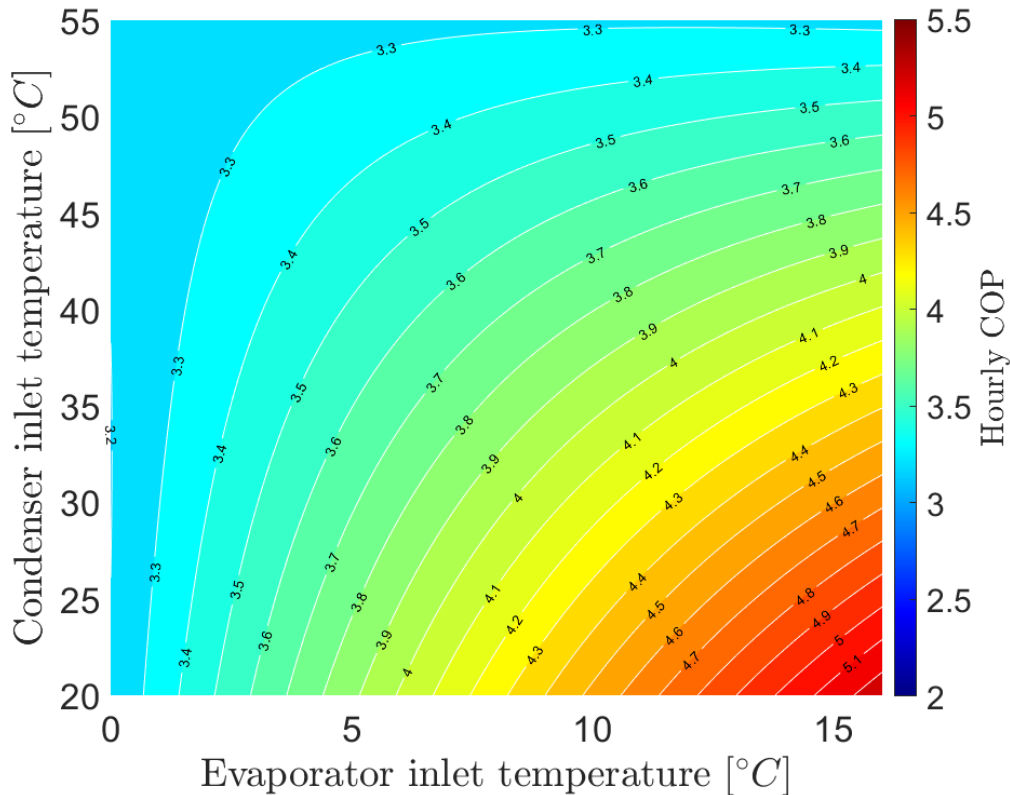


Figure 23. Fitted performance map of the heat pumps' COP

Note that the manufacturer rated COPs are of 4.33 and 2.86 for temperature levels of 0/-3°C – 30/35°C and 0/-3°C – 47/55°C. The Monthly Performance Factors (MPFs) of the heat pumps (MPF₁) during the monitoring period are presented in Figure 24. The MPFs appear quite stable over time, without any large difference between summer and winter periods. A possible explanation is that COP during space heating production is higher than during DHW production. So, although the source temperature is lower during the winter period (see Figure 16), lower condensation inlet temperature due to more space heating production act as a compensation for the PFs. This is particularly visible for the months of September and October which are the first months with space heating needs and also show a small step in PF compared to previous months.



Figure 24. Monthly Performance Factor (MPF) of the heat pumps

Overall system performance

The heating MPFs 1, 4, 4+, 5, 5+ and 5* are provided in Figure 25. The assumptions and equations are reminded in part “Performance metrics”. The estimation of the ventilation heat recovery, though uncertain, is included in an alternative performance factor called 5* and the recovered heat is simply added to the numerator (in that case, all the ventilation fan energy is accounted for since heat recovery occurs most of the time). It should be reminded that only a couple of days are included in the months of May 2019 and February 2020.

PF₄ is about 20-23% lower than PF₁ during the summer months while the percentage difference reduces to 14-17% during winter. The difference in percentage may be due to circulation pumps not adapting to the needs. In particular, the brine ventilation pump, the pump discharging heat from the tank to the warm water circulation and the warm water circulation pumps appears to be working almost constantly.

Although they cannot be computed exactly, PF₂ and PF₃ will be within PF₁ and PF₄. For most winter months, this means PF₂ and PF₃ values higher than 3.

There is almost no difference between PF₄ and PF₄⁺. This is because the amount of recovered heat is small in comparison to the total needs but it is not unlikely that the sensor gives an erroneous value, as seen in part “Verifications”. Another reason for which the effect of the wastewater recovery is small is that all cold water is being warmed up, not just cold water meant for DHW. In that way, some of the recovered heat will not be helpful in reducing the DHW needs. The author does not know the reason for this but it seems like a peculiar design choice. Yet another reason might that the heat exchanger bypass is open, which it was at some point in 2018 according to some pictures the author took.

The percentage difference between PF₅ and PF₄/ PF₄⁺ is about 16-19% during winter months while it drops to 1 to 12% summertime. Since space heating needs are almost nil then, ventilation fan energy is not allocated to heating in PF₅. This is made clear by PF₅^{*} which accounts for all fan energy: the latter is low summertime while it is equal or similar to PF₅ during winter.

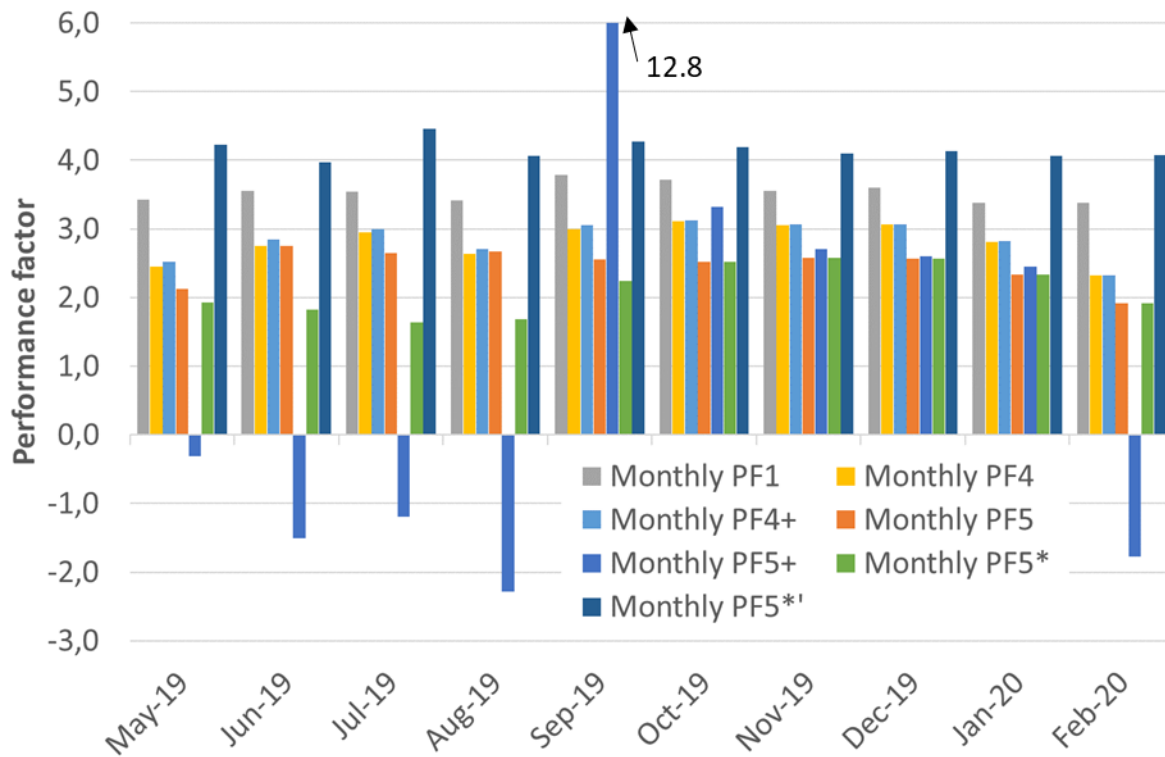


Figure 25. Monthly performance factors for the period May 2019 to February 2020

PF₅⁺ takes into consideration the production from PV cells, hence the sometimes values which mean overproduction (with respect to the energy plant). Three main observations can be made with regard to PF₅⁺. The first one is that there is a significant amount of overproduction summertime. The second one is that the production is very small compared to the needs in winter. This can be seen from PF₅⁺ being similar to PF₅. Note that the negative number from February 2020 is due to that the production from the whole month is accounted while the consumption is only for a couple of days. The third observation is that intermediate months (here September and October) show a proportionally significant amount of PV production. In September, the PV electricity production almost equals the consumption of the energy system which explains the large PF₅⁺ value (12.8).

Including the ventilation heat recovery seems to improve the performance significantly, about 60 to 90% from PF₅⁺ to PF₅⁺* during winter months. Please keep in mind that the heat recovery estimation is more uncertain during summer. PF₅⁺* lie straight above 4 and is fairly constant over time.

It would be of interest to understand how the pre-heating/cooling heat exchanger before the heat recovery exchanger in the AHUs impacts the performance. Fresh air that is first cooled needs to be reheated downstream. At the same time, lowering the fresh air temperature increases the amount of heat that can be recovered in the recovery heat exchanger. This can unfortunately not be calculated yet due to lack of data access.

Temperature measurements from the two AHUs in building 2 indicate that the heat recovery heat exchangers are almost constantly bypassed during winter months. Although it might have, defrosting does not appear to cause this. The reason for this heat recovery bypass is not known but it would be worth investigating to make sure it does not appear next winter. This should be kept in mind when looking at PF₅⁺.

Another way to represent performance is to split up the energy items making up the different performance factors, separating between delivered energy and consumption. Such a figure is represented in Figure 26 with PFs 1,4,4⁺,5 and 5^{*}. The production from PV cells is also included and split between self-consumption and overproduction (from the energy plant standpoint). In combination with the PF values, the split-up may help understand the differences and what consumption or production items may be reduced or increased in order to improve performance.

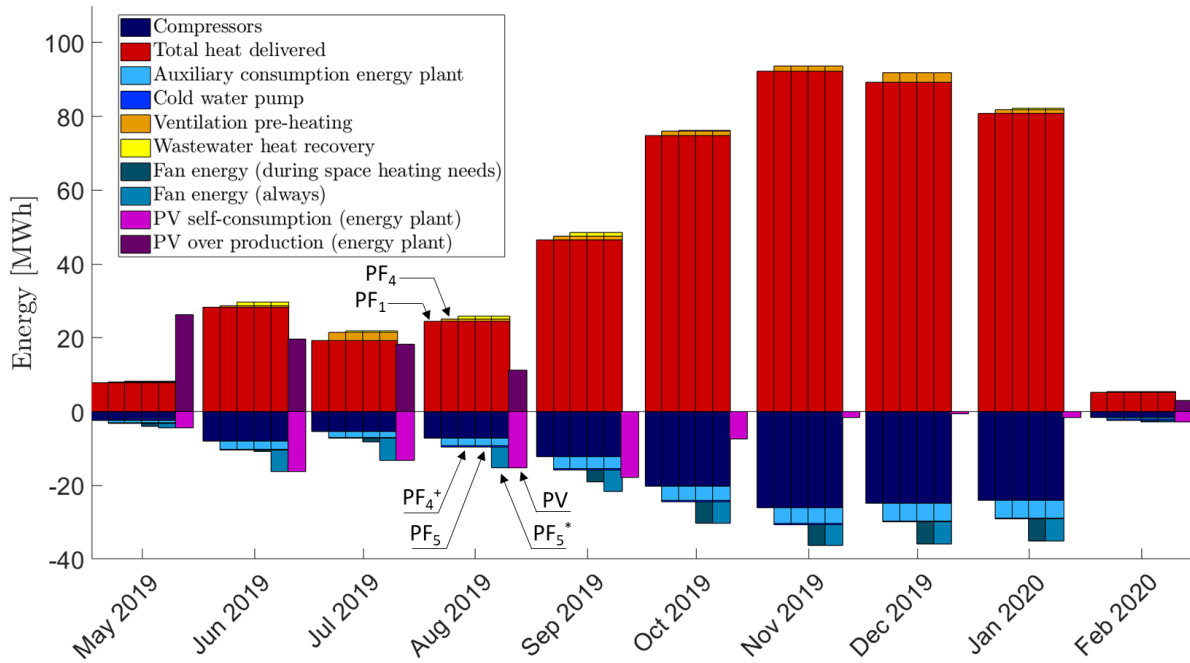


Figure 26. Energy split-up for different performance factors

Electricity consumptions for different parts of the buildings are available over nearly two years. These are plotted in Figure 27 with the consumption plotted in the foreground and the production or bought electricity are plotted in the background.

The electricity consumption of the ground source heat pump system dominates the consumption overall and more specifically during winter. The electricity usage of the GSHP system is assumed to include the circulation pumps and this is checked by comparing the heat pump energy and auxiliary consumption of the energy plant to the GSHP electricity usage (these appear as three different sensors in the data). The difference is always lower than 1.6% with the exception of June 2019 (~7%).

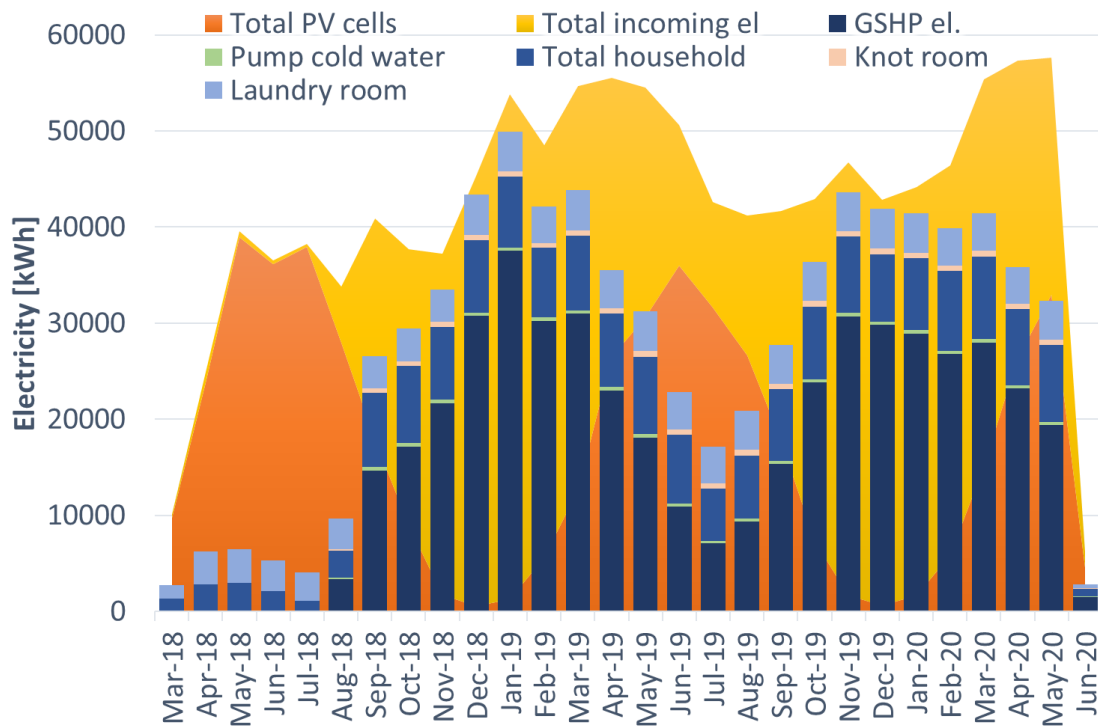


Figure 27. Monthly electricity consumption and production

As can be seen in GSHP Figure 27 electricity consumption data are missing for the first months of operation. The consumption of the cold water pump and the “knot room” (the author is unsure about what this is, perhaps a server room?) are small in comparison to the total consumption. On the other hand, the electricity use for the laundry room and the households have a rather large share. It is unclear if the fans’ energy is included in the household consumption.

Figure 27 also highlights the mismatch between PV cells production and electricity usage throughout the year. More surprisingly is the fact that electricity is bought during the summer (2019) although the PV cells production exceed the consumption. This is due to daily mismatch between production and consumption: the GSHP system works at night when the sun is not shining. This daily mismatch is not noticed for monthly aggregated data. In addition, the PV cells production may be specific to each house, i.e. if the PV cell production from house 2 (where the heat pumps are installed) does not suffice: electricity is bought from the network although the other two houses have excess production.

The PV panels were designed to produce about 217 MWh per year and data shows a yearly average of 209 MWh. The difference may be due to variation in yearly solar flux. Considering that the 667 solar panels have a standard area of 1.67 m² (8x12 cells), the amount of produced energy per square meter of panel is 185 kWh/ m². The inclination of the solar panels is not known but from pictures they appear to have a rather low inclination. This allows for more PV area to be installed but this is not optimized for production during winter months, when the sun is low and the heat demand is large.

The three buildings are designed as plus-energy houses so they are supposed to produce more energy than they consume (not including the individual energy consumption). Data for three different yearly periods however show a clear deficit: 75.3 MWh for the period September 2018 – August 2019, 92.2 MWh for the year 2019 and 54.5 MWh for the period May 2019 to June 2020.

Table 9 provides a summary of the different energy figures used for the calculation of the performance factors as well as the electricity consumption and production figures for the longer monitored period. Table 10 shows the different performance factors and their 95% confidence level uncertainty for the whole monitored period. Table 11 shows additional performance indicators.

Table 9. Provided heating, cooling and used electricity

Start of evaluation period	2019-05-26	2018-03-01	2019-01-01	2020-01-01
End of evaluation period	2020-02-03	2018-12-31	2019-12-31	2020-06-03
Heat output from the ground source, used by heat pump for heating [kWh]	247,406			
Heat output from the heat pump [kWh]	468,641			
Heat recovered from wastewater (boundary 4+) [kWh]	3,909			
Fresh air pre-heating in ventilation system (boundary 4) [kWh]	10,890			
Estimated heat recovery from the ventilation (boundary 5*) [kWh]	391,148			
Cooling output from the ground source (recharge) [kWh]	74,246			
Electricity used by the heat pump compressor, including internal control system [kWh]	131,556			
Electricity used by all source and load side circulation pumps (boundary 4) [kWh]	27,905			
Cold water pressurizer (boundary 4) [kWh]	3,334 ¹	1,587	4,110	1,726
AHUs’ fans electricity use during heating (boundary 5) [kWh]	29,210			
AHUs’ fans electricity use continuously (boundary 5*) [kWh]	48,400			
PV cells electricity production (boundary 5+) [kWh]	159,715 ¹	203,565	198,153	86,388
Electricity used by the GSHP system [kWh]	200,663 ¹	87,610 ²	266,687	127,807
Electricity used by the households [kWh]	72,998 ¹	43,914	87,056	41,155
Electricity used by the “knot room” [kWh]	5,775 ¹	2,265	6,888	2,861
Electricity used by the laundry room [kWh]	40,319 ¹	31,936	48,397	20,136
Bought electricity [kWh]	293,783 ¹	140,731	377,373	180,742

¹Includes the whole May 2019 and February 2020 months.

²No data until 2018-08-24.

Table 10. Performance factors over the monitoring period with 95% uncertainty bounds

Start of evaluation period	2019-05-26
End of evaluation period	2020-02-03
PFH1 ¹	3.56 ±0.09
PFH4	2.95 ±0.28
PFH4+	2.97 ±0.28
PFH5	2.52 ±0.24
PFH5+	14.97 ±1.92
PFH5*	2.29 ±0.22
PFH5**	4.14

¹heat pump internal electricity use is included.

Table 11. Additional performance indicators

Start of evaluation period	2019-05-26	2018-03-20
End of evaluation period	2020-02-03	2020-06-01
Ratio of auxiliary electricity (circ. pumps) to heat pump electricity [%]	21.2%	-
Mean heat exchange per unit length of borehole heat exchanger, heating [W/m] (energy [kWh/m])	21.2 (80.2)	-
Mean heat exchange per unit length of borehole heat exchanger, recharge [W/m] (energy [kWh/m])	12.0 (24.1)	-
Energy system heating demand per heated surface area per year [kWh/(m ² yr)]	66.0 ¹	-
Building heating demand (including ventilation heat recovery) per heated surface area per year [kWh/(m ² yr)]	119.4 ¹	-
PV electricity production per panel area per year [kWh/(m ² yr)]	170 ¹	185
Electricity net consumption per year [kWh/yr] (excluding individual electrical cons.)	27,010 ¹	16,549

¹Figures obtained by normalizing the monitored period to a full year

Uncertainty analysis

In the uncertainty guidelines associated with the IEA HPT Annex 52 project, it is explained that random errors will become negligible when aggregating data over a large period of time (typically a month or a year). This stems from the law of large number in statistics. The main contributors to the uncertainty of the different performance factors are systematic errors, or rather the mean value of systematic errors over the period of interest. Variations around this mean will tend to become negligible for just the same reason that random errors are negligible (unless the variations are very large).

Now, if systematic errors are known, one should simply correct the measurements to cancel their effect. What we should assume then is that uncertainty stems from potential systematic errors or systematic errors which correction is too tedious to calculate or implement. Since these are unknown, they can be modelled as a random variable but not one which outcome changes in time. The mean of an “uncertain systematic error” must be zero (otherwise, one should just correct the measurement) and its distribution characterises – loosely said – how likely it is that it will take a certain value other than zero (based on quantitative and/or qualitative approaches).

It is believed that manufacturers report accuracy in a similar way: rather than calibrating every sensor, a representative sample is tested from which an error distribution is inferred and checked against a norm. Thus, the accuracy reported by manufacturers is an indication of a sensor may systematically measure a value, say, 2% higher than the true value, rather than an indication of how measurements from a given sensor will vary around the true value (random error). To be fair, random errors are also included in the accuracy reported but they are usually smaller than potential systematic errors. Note that some manufacturers may also test and calibrate each sensor (e.g. some flowmeters), in which case random errors can be dominant in the reported accuracy. Usually, only one value is given for the accuracy without any indication about the distribution or confidence level at which this value is given. In many cases, the given value corresponds to a maximum permissible error and it is defined according to a norm. In the absence of any other information, error might be assumed to be normally distributed and the accuracy given for a 95% confidence level. Here however, we will assume uniform distribution to be more conservative.

This rather long introduction serves three purposes. Firstly, potential/unknown systematic errors will dominate performance factor uncertainty. Secondly, accuracy given by the manufacturer may be used for uncertainty analysis since it mainly represents systematic errors (except for specific cases). Thirdly, the accuracy may be interpreted as the low and upper bound of a uniform continuous distribution, which characterize the potential systematic error(s).

In the Annex 52 uncertainty guidelines, error values are combined regardless of the underlying distribution and what the error value actually represent (upper bound of a uniform distribution, standard deviation, 95% confidence level, etc.). This is fine but may lead to overestimated uncertainties (this follows from the central limit theorem). Here, we will follow recommendations from the Guide to the expression of Uncertainty in Measurement (GUM) [7], namely to determine standard combined uncertainties based on standard deviation values and propagation of error. The standard combined uncertainty may then be expanded with a coverage factor corresponding to a confidence level.

For example, for PF_1 , the propagation of error leads to

$$\frac{u(PF_1)}{PF_1} = \sqrt{\frac{u^2(Q_{HP,tot})}{Q_{HP,tot}^2} + \frac{u^2(W_{HP,tot})}{W_{HP,tot}^2}} \quad (9)$$

where u 's are standard uncertainties (standard deviations).

The total amount of heat delivered by the heat pump may be expressed as

$$Q_{HP,tot} = \sum_i Q_{desup,DHW,i} + Q_{cond,DHW,i} + Q_{cond,sH,i} \quad (10)$$

Each component's contribution is then summed in quadrature as follows

$$u(Q_{HP,tot}) = \sqrt{u^2(Q_{desup,DHW}) + u^2(Q_{cond,DHW}) + u^2(Q_{cond,SH})} \quad (11)$$

where u 's are the standard uncertainty values, accounting for the manufacturer's specified accuracy, here $(0.15 + \frac{2}{\Delta T_i})\%$ and to potential systematic errors that may arise independently from the meter itself, for instance heat losses/gains between the heat pumps and the meter, sensor bias due to position (e.g. in thermo-pockets), errors to shocks and vibrations, etc. Here the distribution of extra potential systematic errors is taken uniform with a 2% high bound. N is the number of measurement points in the aggregated period.

Now, to determine the u^2 's is non-trivial since the standard uncertainty of their underlying components is changing at every time steps. When adding random variables that produce an outcome (drawn for their distribution) at every time step, their standard deviations should simply be added in quadrature. Here, however, the systematic errors are not drawn at every time step, so how should the standard uncertainty of the sum be computed? As previously alluded to, variations will tend to vanish when they are aggregated over time so only the mean systematic error in time will remain⁴. Hence, the uncertainty of the sum is the sum of the standard uncertainties for each component

$$\bar{u} = \frac{1}{\sqrt{3}} \sum_i \frac{|Q_i|}{100} \sqrt{\left(0.15 + \frac{2}{\Delta T_i}\right)^2 + 2^2} \quad (12)$$

Note that the factor $\sqrt{3}$ comes from the fact that error distributions are assumed uniform.

The relative standard uncertainty of the heat pump power measurements is not known but is constant assumed as 2% (high bound of uniform distribution). The standard uncertainty of the total energy consumption may then be calculated in similar way as for the total heat rate, giving

$$u(W_{HP,tot}) = \frac{0.02}{\sqrt{3}} \sqrt{W_{HP,1}^2 + W_{HP,2}^2 + W_{HP,3}^2} \quad (13)$$

The expanded uncertainty of PF_1 may then be computed as

$$U(PF_1) = c_{1-\alpha} \left(\frac{u(PF_1)}{PF_1} \right) PF_1 \quad (14)$$

where $c_{1-\alpha}$ is the coverage factor for a given significance level α (or confidence level $1 - \alpha$). $c_{1-\alpha}$ is calculated assuming a normal distribution (1.96 for 95% confidence level). The degree of freedom is implicitly assumed to be infinite.

The uncertainty of other performance factors may be calculated in the same way. Namely, propagation of error is applied to the performance factor formula and then each term's standard uncertainty is determined, keeping in mind that uncertainties over time are not added in quadrature but "regularly" (since the (mean) systematic error does not change in time).

In the absence of further information, all electrical consumptions are assumed to have the same relative standard uncertainty ($\frac{0.02}{\sqrt{3}}\%$). For PF_4 , the relative standard uncertainty of ventilation pre-heating may be assessed as

$$\delta u_{vent,preheating}^2 = \delta u^2(\dot{V}) + \delta u^2(\rho) + \delta u^2(c) + \delta u^2(\Delta T) \quad (15)$$

⁴ We must clarify that systematic errors that vary in time have three different elements to them: 1) the overall mean (or expectation), 2) the mean systematic error with respect to time and 3) the variations in time. Elements 2 and 3 have their own distribution that occur in two different "spaces". We previously wrote that: "The mean of an "uncertain systematic error" must be zero" but this refers to the first element, which by the way is the mean of the mean with respect to time.

The density and specific heat capacity relative standard uncertainty are considered negligible ($\delta u^2(\dot{V})$ is large). The standard uncertainty of the temperature difference may be expressed as

$$u^2(\Delta T = T_1 - T_2) = u^2(T_1) + u^2(T_2) \tag{16}$$

with the singular temperature standard uncertainty obtained from manufacturers' specification (see Table 6). Temperature measurements are assumed uncorrelated to be conservative. The volume flow rate estimation is based on many different calculations, which makes it very cumbersome to calculate. Data suggest that the relative standard uncertainty is very high, about 50%.

Since PF₄ also includes the storage tanks, one should include the potential difference in DHW production highlighted in Figure 12. The relative standard deviation of the differences is about 14.2% so this value is included in eq.(12) for the condenser and desuperheater DHW production (added in quadrature and assumed to have a uniform distribution).

The monthly performance factors and their corresponding 95% confidence level uncertainty are presented in Figure 28. Uncertainty for the whole monitored period may be found in Table 10 presented earlier in this document.

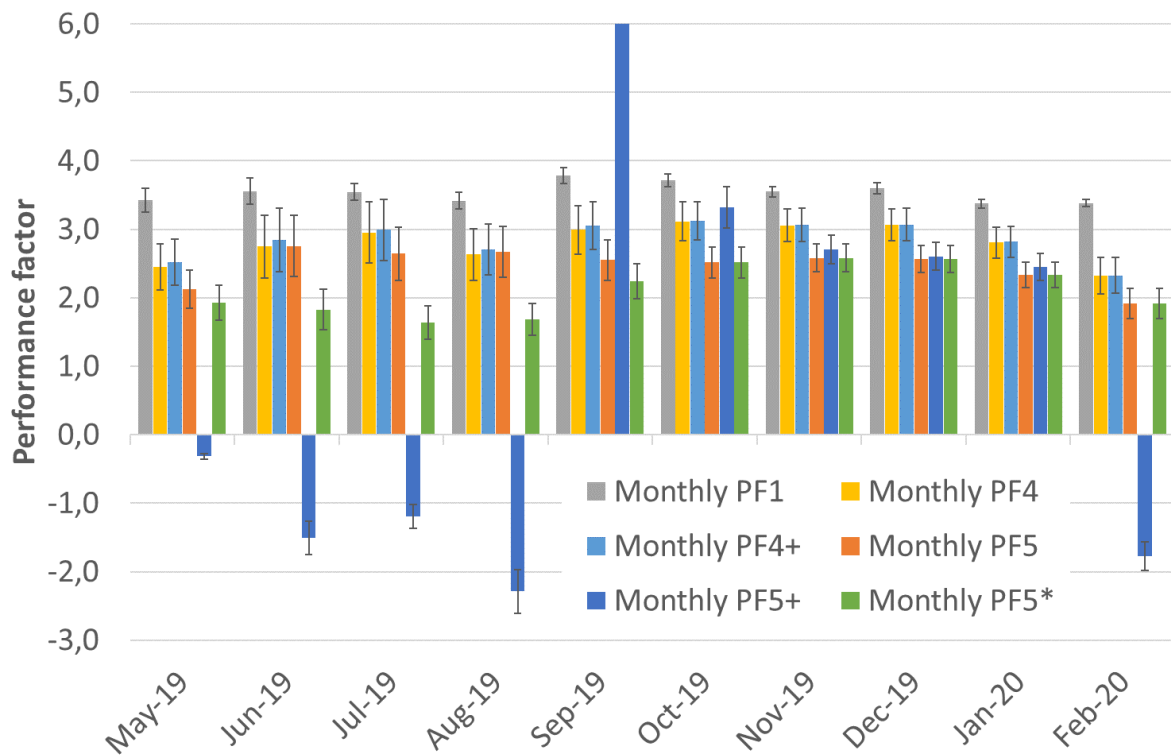


Figure 28. Monthly performance factors and their 95% confidence level uncertainty for the period May 2019 to February 2020

LESSONS LEARNT

Design lessons learnt

High pressure in the brine loop

During on-site visits, before measurement data was available, an abnormally high pressure (about 7 bar) was noticed on the display of circulation pump placed on the source side of the heat pump. This came for a differential pressure measurement, which the pump uses for controls. After verifications with on-site manual manometers, it appears that high pressure did occur in source side loop close to the heat pump as shown in Figure 29. This issue only appeared when the circulation pump was not operating.

Looking at data, it appears that this issue is frequent as can be observe on Figure 30. The pipes have a pressure rating of PN10 so they can withstand 10 bar (here corresponding to about 8.8 bar in differential pressure). From Figure 30, it appears that this limit is not rarely close or at the limit.

It is believed that this issue is caused by thermal expansion of the fluid when the valves SV11, SV12, SV13 and KB1-SV10 are all fully closed. In that case, the part of the circuit circled in red in Figure 29 will be disconnected from the expansion vessel and pressure will build up in the closed circuit. This is consistent with Figure 30 which shows that the issue occur more frequently during the summer, when the heat pumps are operated more seldom.

This issue could be fixed by adding a static connection line to the expansion vessel⁵.

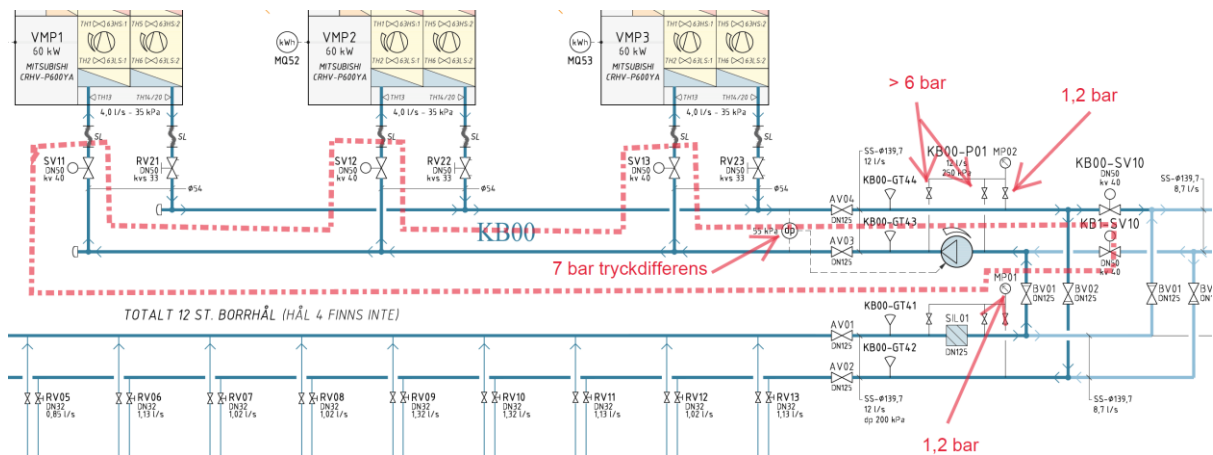


Figure 29. Snapshot of the hydraulic flowchart showing where the high pressure occur (courtesy of Enstar)

⁵ The building owner and the installer were contacted but they have not yet acted on the matter as far as the author knows.

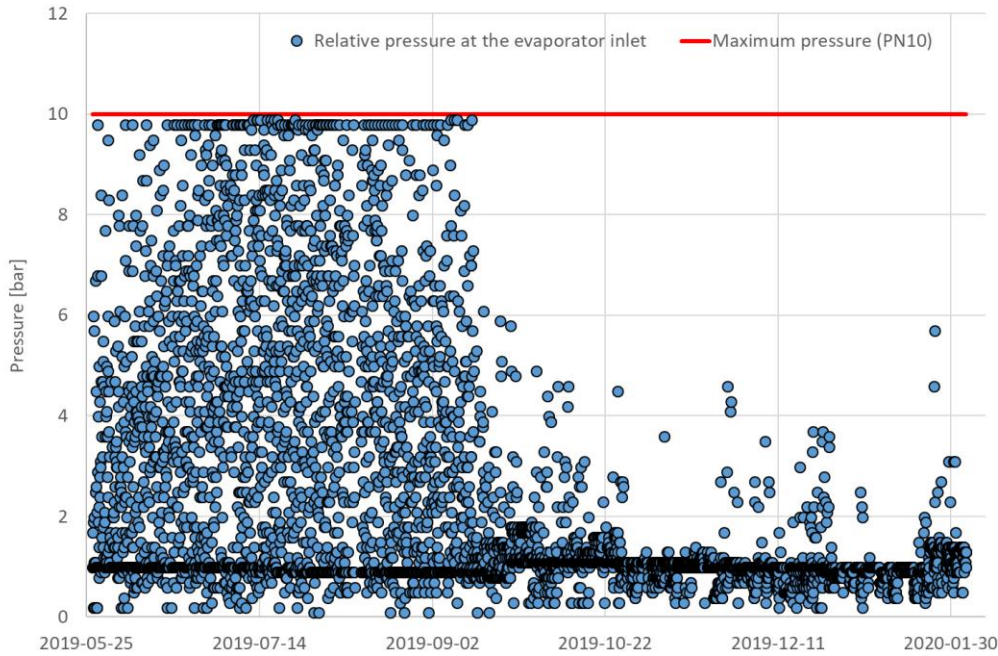


Figure 30. Relative pressure at evaporators' inlet during the monitoring period

Recharging the boreholes through the ventilation

Does it make sense to cool down the fresh incoming air – thereby recharging the boreholes – when the buildings have heating needs? In such case, the fresh air is first cooled down, then it recovers heat in the recovery heat exchanger before being warmed up to a suitable temperature and supplied to the building. In principle, this is no different from electrical heating. Accounting for losses (heat losses, circulation, etc.), it is even less efficient.

One potential advantage with this setup, however, is that it may increase the amount of heat recovered through the recovery heat exchanger. This is because a lower air inlet temperature increases the potential for heat transfer. From a theoretical standpoint, this can be understood by the following reasoning. First, the effectiveness of the recovery heat exchangers may be expressed as

$$\varepsilon = \frac{C_h(T_{h,i} - T_{h,o})}{C_{min}(T_{h,i} - T_{c,i})} = \frac{C_c(T_{c,o} - T_{c,i})}{C_{min}(T_{h,i} - T_{c,i})} \quad (17)$$

where $C = \dot{m}c$ is the heat capacity rate, the subscripts h and c refer to the hot and cold side and the subscripts i and o refer to inlet and outlet, respectively. $C_{min} = \min(C_h, C_c)$. Here, since the flow rates and thermal properties are similar, we can make the simplification that $C_h \approx C_c$, which simplifies eq.(17). On the other hand, the effectiveness is only a function of the NTU number and the ratio of heat capacity rates

$$\varepsilon = f\left(NTU = \frac{UA}{C_{min}}, \frac{C_{min}}{C_{max}}\right) \quad (18)$$

Thus, for a given heat exchanger and given flow rates, the effectiveness will be constant if the change in thermal properties can be neglected. Then, using eq.(17), it can be shown that the difference in recovered power is

$$\Delta\dot{Q} = \varepsilon\Delta T_{inlet}C_c = \varepsilon\dot{Q}_{recharge} \quad (19)$$

with ΔT_{inlet} the difference in inlet temperature caused by the heat exchanger upstream of the recovery heat exchanger and $\dot{Q}_{recharge}$ the amount of power exchange in the upstream heat exchanger. Note that this is valid for no bypass flow, which was also implicit in saying that $C_h \approx C_c$.

This corresponds to a performance of

$$PF_1' = (1 - \xi)(1 - \varepsilon) + \varepsilon PF_1 \quad (20)$$

where ξ is the compressor heat losses (see part “Performance calculation lessons learnt” for further explanations). If ε is nil (no heat recovery), the performance is slightly lower than 1 so slightly worse than electrical heating. If ε is equal to one, then the performance of the heat pump is unchanged but the boreholes are recharged. It is expected that effectiveness should be between 80 to 95% so a good approximation is $PF_1' \approx \varepsilon PF_1$. With this performance estimation, it appears that it makes sense to recharge the boreholes through the incoming air. Obviously, circulation pumps should also be accounted for in the performance but it is believed that the solution would be viable even then.

Moreover, lower inlet temperatures to the heat recovery exchanger will favor condensation on the return air side, which would further increase the amount of heat recovered. One potential disadvantage is that the need for defrosting might increase if boreholes are recharged during cold winter days. However, no extra defrosting need was noticed during the monitored period.

Another advantage of having a pre-heating / recharging heat exchanger is that it allows to provide some comfort cooling during summer (although condensation may lead to slightly dry supplied air). An alternative to recharge the boreholes through the fresh air is to charge them through the exhaust air (after heat recovery). The temperature is almost always higher, it does not create any extra heating needs and does not increase the risk of defrosting requirements. On the other hand, no cooling could be provided in that way.

The analysis presented here remains theoretical and data would be needed to support the argumentation. Nevertheless, it appears to be a good design choice to recharge the borehole through the fresh incoming air if a ventilation heat recovery unit is used.

Performance calculation lessons learnt

Compressor heat losses and evaporator heat estimation

The ratio of condenser to evaporator heat $\beta_{HP} = Q_1/Q_2$ is often taken as $\frac{SPF_1}{SPF_1-1}$ where $SPF_1 = \frac{Q_1}{W_{el}}$ is the Seasonal Performance Factor of the heat pump unit, i.e. the ratio between the compressor energy consumption, W_{el} , and the heat delivered by the heat pump (the reasoning is the same if one consider the COP instead). This equation, however, only true for (semi-)hermetic, adiabatic compressors.

The first law of thermodynamics tells us that $Q_2 + W_f = Q_1$ where Q_2 is the heat absorbed at the evaporator, Q_1 is the heat rejected at the condenser and W_f is the energy provided to the refrigerant in the compressor. If the compression is not reversible, W_f will be the sum of the isentropic work and some friction heat generated in the process.

The expression $\frac{SPF_1}{SPF_1-1} = \beta_{HP}$ can be derived from $Q_2 + W_f = Q_1$ only if $W_f = W_{el}$. The latter only occur is all the electrical losses are recovered by the refrigerant. This might be true for hermetic or semi-hermetic compressors in which the motor is cooled down by the refrigerant. The compressor envelop must, however, be adiabatic; the hot, compressed refrigerant will otherwise lose heat to the environment. If heat is lost by the refrigerant to the surroundings, the energy balance becomes $Q_2 + W_{el}(1 - \xi) = Q_1$ where ξ is the percent heat loss, usually about 5-10%. For open compressors, this figure will be even be higher. The previous equation can be modified to obtain $\beta_{HP} = \frac{SPF_1}{SPF_1-1+\xi}$. Neglecting the heat losses may lead to about 5% overestimation of β_{HP} , which in turn leads to an underestimation of Q_2 .

It may be rightfully argued that the heat lost through the compressor envelop participate in heating the building. If so, one may define β'_{HP} as $\frac{Q_1+\xi W_{el}}{Q_2}$ and $SPF'_1 = \frac{Q_1+\xi W_{el}}{W_{el}}$, which leads to $\beta_{HP} = \frac{SPF'_1-2\xi}{SPF'_1-1-2\xi}$.

A somewhat similar discussion is provided in Granryd et al.[8] for refrigeration units (see chapter 7 A2).

Uncertainty related to the sampling frequency

During the course of Annex 52, some discussions have arose about what sampling frequency is suitable for measuring the performance of the GSHP systems and associated buildings. In the Forsknigen buildings, data are gathered every minute. Most of these data are unfortunately not available to the author, but some electricity consumptions are. The energy consumption of the GSHP system is used to test different sampling frequency during the period 2018-03-20 to 2020-03-17 (nearly two years). Now, energy are usually aggregated over time and the issue of the sampling frequency rather apply to non-aggregated data. Thus, the energy values are first converted into power values to mimic a sensor measuring non-aggregated values. The results are presented in Figure 31 that shows the percentage error for different sampling intervals, compared to one minute sampling interval.

It is hard to find a clear pattern but the absolute value of the error appears to increase for larger sampling intervals (lower sampling frequency) in average. Having a relatively small sampling interval is not necessarily a guarantee of low error value. Here for instance, a sampling interval of 15 min leads to an error of about 2.7%.

Results presented here are valid for this specific case only and the reader is referred to the Annex 52 uncertainty guidelines for more in depth discussions about this potential issue.

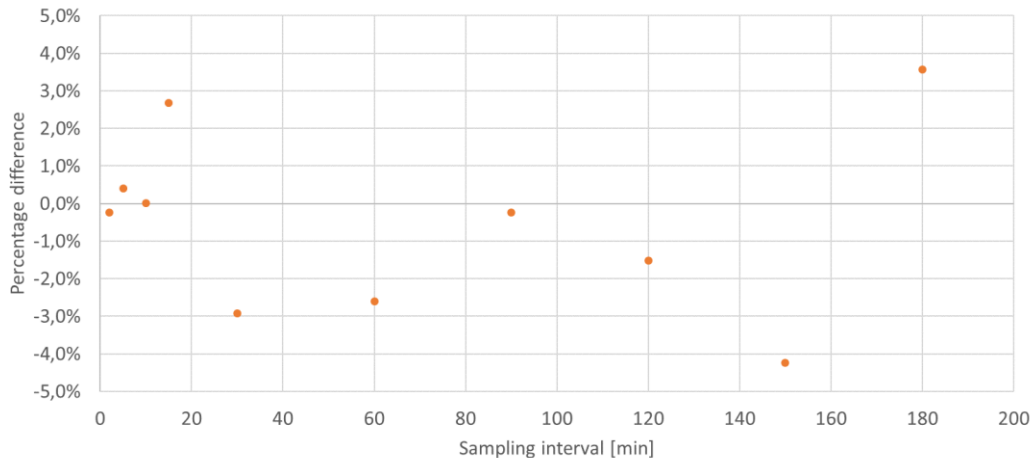


Figure 31. Percentage related to different sampling frequency for non-aggregated data

Data quality and verifications

Here we just want to remind the conclusion from the part “Verifications”. Namely, that data cannot be blindly trusted and require a minimum level of interpretation. Looking at coarse-grained aggregated data (yearly) may lead to missing some data inconsistencies.

Average COP is not the same as SPF

This may read as obvious for some, but average COP is not the same as SPF. The SPF is a weighted COP average

$$SPF = \frac{Q}{W} = \frac{\sum_i Q_i}{\sum_i W_i} = \frac{\sum_i COP_i \cdot W_i}{\sum_i W_i} \quad (21)$$

Thus, SPF is a better indicator of the system performance as it naturally weights performance with the amount of electricity used whereas all COPs have the same weight in the average COP value. Hence,

the COP during an hour or day with low energy needs may have too large of a role in the average COP and create a bias in the performance indication. For instance, for the installation at hand in this report, the average COP tends to be lower than the SPF because the COP during DHW production summertime (when the total heat demand is lower) is usually lower than when space heating is required (wintertime).

Improvement measures

Here is a – probably non-exhaustive – list of measures that have a potential to improve the performance of the energy system and that would be worth investigating further:

1. Check why the heat recovery exchangers in the AHU 2 and 3 are bypassed.

During winter, the heat recovery exchangers in the ventilation of building 2 appear to be partly bypassed. The reason for this is not fully clear but it does not appear to be because of defrosting needs. Is it a control issue or an issue with the by-pass dampers or something else? The author does not know but amount of heat that could have been recovered is very large and the effort to fix the issue seems more than reasonable. This can be seen in Figure 14, which already accounts for this bypass issue. Thus, the ratio between heat recovered from the ventilation and heat provided by GSHPs could be even lower.

2. Brine circulation to the ventilation AHUs always on

As the sub-title suggests, the circulation pump bringing brine to the pre-heating/recharging heat exchanger in the ventilation AHUs is almost always on. Is this done for control reasons (in which case it could be improved) or because there are always pre-heating / recharging needs? This should better understood and corrected if need be

3. Brine circulation pumps frequency-control based on constant ΔP

Both circulation pumps in the GHE loop are frequency-controlled based on a constant ΔP set point. This is a good way to control these pumps, especially since there are control valves that closes when the different equipment are no used, e.g. if only heat pump 2 operates, no circulation occur in heat pumps 1 and 3. Nevertheless, the heat pump units themselves have two refrigeration cycles and each compressor has variable speed so the flow rate provided by the circulation pump does not adapt to the actual heating need. It is the author's belief that a control based on ΔT (evaporator inlet/outlet temperature difference for the heat pumps) would lead to better performance as it adapts to the needs. For heat pumps, a temperature difference of 3 K is usually taken as set point. For the pre-heating/recharging heat exchanger in the AHUs however, the optimal set point should be investigated.

4. Space heating booster pumps always on simultaneously

Besides the main space heating circulation pump, each building has its own “booster” pump supposedly to adjust the flow rate based on the needs. The data indicate that all three pumps are always running simultaneously, which may be a control pitfall.

5. DHW storage tank heat losses

It was seen in Figure 12 that there appears to be a significant difference between charged and discharged energy from the DHW tanks. Monthly differences are negative for the most part but not always. In any case, it is believed that heat losses from the DHW storage tanks may be playing a role there. The 8 tanks are placed in a large room which is mostly empty so there is no thermal mass that could dampen the heat losses. A check on site proved that the surface temperature of the insulation was quite warm, indicating that heat losses do occur at non-negligible rate.

6. DHW expansion into space heating loop

The DHW and space heating loops share the same expansion tank, which is placed in the space heating loop. Therefore, an expansion connection with a check valve exists between the two loops allowing

water to expand but not pass through under “normal” circulation conditions. As seen in Figure 32, this “expansion leakage” maintains the heat pump return temperature from the space heating storage tanks at around 45°C during summer, when space heating needs are almost non-existent (the few times that needs occur is actually when the temperature drops). The supply temperature is not affected as much because the expanded water has to travel a longer distance to reach it. Although the amount of heat lost is not known, this issue could be easily fixed by setting up a new expansion tank.

This point could as well as have been raised under part “Design lessons learnt”.

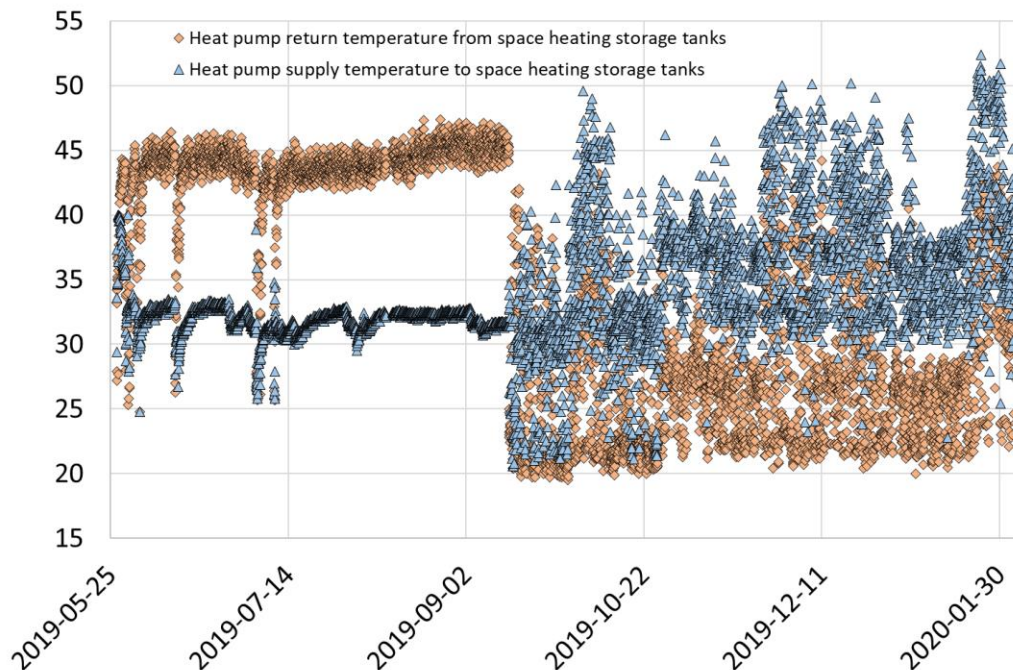


Figure 32. Heat pump return and supply temperatures from/to the space heating storage tanks

7. Wastewater heat recovery for DHW only?

The wastewater heat recovery heat exchanger warms the incoming cold water that is for both DHW and apartments’ cold water, supplying at around 14°C in average (instead of 11°C). The reason for warming up even the cold water no used for DHW in fine is not known but the author believe that it would be better to have a design that just pre-heat the cold water meant for DHW use. As for the previous point, this point could as well as have been raised under part “Design lessons learnt”.

8. Mixing cold water with re-warmed DHW circulation?

There are two heat exchangers for the DHW production: one warms (pre-heated) cold water up and the other one warms the DHW circulation up. However, the outlet of the second heat exchanger is connected with the inlet of the first one. The author believes that this is a mistake and the supposed reason is that traditional DHW production with circulation only includes one heat exchanger. In the traditional solution, the DHW circulation must then be mixed with cold water before being warmed in the heat exchanger. With two heat exchangers however, the outlets of each heat exchanger can be mixed and no mixing should be required at the inlets. If such a solution would be implemented, it is believed that the return temperature from the main exchanger would be lower, hence allowing for more heat to be stored in the tank and improving the heat pumps’ performance.

9. Desuperheater loop mixing with condenser

This is somewhat similar to the previous issue. The three heat pumps are equipped with a desuperheater. This is a priori good: it allows producing heat at higher temperatures, which is useful to cover DHW for instance. Nevertheless, the heat production from the desuperheaters is mixed with that of the condensers before going to the storage tanks. The usefulness of the desuperheaters is thereby diminished. Since there is a segregation between the desuperheater loop and condenser loop for the

return lines (for charging operation, the desuperheaters charge the two warmest tanks), it is unfortunate that the segregation does not exist for the supply lines.

10. PV cells and battery

As seen in part “Overall system performance”, there is a seasonally, monthly, daily and even hourly mismatch between PV production and electricity consumption. It may be worth to investigate if batteries could help reduce the daily and hourly mismatch, especially in house 2 where the consumption is high due to the heat pumps. In fact, a research project in which batteries will be coupled to the PV panels of this property will start in 2022.

Future work

Besides following-up on the improvement measures listed in the previous section, more long-term data would need be analyzed to strengthen the analysis presented in this report (at least a full year period). The author sees gaining access to raw data (minutely data) from all the sensors as the absolute top priority for deepening the work presented in this report, both from academic and practical standpoints.

Coupling the energy system analysis to a building/apartments analysis and occupants’ feedback could be an interesting way forward, especially since the individual apartments are well-equipped with sensors.

The author believes that there is always some degree of interpretation involved in performance analysis and investigating what performance different people find would be an interesting thing per say.

The report highlights the gap between design (plus energy) and actual performance (energy deficit) for a specific case. It would be very interesting to conduct such comparison for other types of buildings. The author believes that such design/performance gaps are usual.

Finally and more generally, the type of performance analysis presented in this reported in quite time consuming and the whole building sector would benefit from having – at least part of – the performance analysis automatized. According to the author’s experience, it is not seldom that building owners have stored data that is not used (perhaps because it is hard to find a viable business case for it).

REFERENCES

- [1] SMHI, “Ladda ner meteorologiska observationer | SMHI,” 2021. <https://www.smhi.se/data/meteorologi/ladda-ner-meteorologiska-observationer#param=airtemperatureInstant,stations=all> (accessed Oct. 05, 2021).
- [2] A. Moberg, “Stockholm Historical Weather Observations — Daily mean air temperatures since 1756 | Bolin Centre Database,” Jan. 29, 2020. <https://doi.org/10.17043/stockholm-historical-temps-daily-2> (accessed Oct. 05, 2021).
- [3] S. Poppi, N. Sommerfeldt, C. Bales, H. Madani, and P. Lundqvist, “Techno-economic review of solar heat pump systems for residential heating applications,” *Renewable and Sustainable Energy Reviews*, vol. 81, pp. 22–32, Jan. 2018, doi: 10.1016/j.rser.2017.07.041.
- [4] N. Sommerfeldt and H. Madani, “In-depth techno-economic analysis of PV/Thermal plus ground source heat pump systems for multi-family houses in a heating dominated climate,” *Solar Energy*, vol. 190, pp. 44–62, Sep. 2019, doi: 10.1016/j.solener.2019.07.080.
- [5] I. Malenković, P. Pärtsch, S. Eicher, J. Bony, and M. Hartl, “Performance and its assessment,” in *Solar and Heat Pump Systems for Residential Buildings*, John Wiley & Sons, Ltd, 2015, pp. 63–102. doi: 10.1002/9783433604830.ch04.
- [6] Å. Melinder, “Thermophysical Properties of Aqueous Solutions Used as Secondary Working Fluids,” PhD Thesis, 2007. Accessed: Mar. 26, 2018. [Online]. Available: <http://urn.kb.se/resolve?urn=urn:nbn:se:kth:diva-4406>
- [7] JCGM, “Evaluation of measurement data — Guide to the expression of uncertainty in measurement,” Joint Committee for Guides in Metrology, 100:2008, 2008. Accessed: Apr. 11, 2017. [Online]. Available: <http://digilib.uin-suka.ac.id/10881/>
- [8] E. Granryd, I. Ekroth, P. Lundqvist, Å. Melinder, B. Palm, and P. Rohlin, *Refrigeration Engineering*. Stockholm: Department of Energy Technology Division of Applied Thermodynamics and Refrigeration Royal Institute of Technology, KTH, 2011.

Project data access

It is the author’s intention that data used to make this work should be available for all. There have been, however, several issues with getting access to data due a complicated data ownership scheme. In addition, other research projects are on-going at the same site, so the best for anyone that get access to data is to contact the author so that data can hopefully be shared without any complications.

Project participants and their contribution

Willem Mazzotti Pallard: methodology, software/coding, database, validation, analysis, investigation, writing, visualization.

Alberto Lazzarotto: methodology, software/coding, investigation, supervision.

Mohammad Abuasbeh: methodology, investigation.

José Acuña: methodology, investigation, supervision, project administration, funding.

Signhild Gehlin: project administration, funding.

APPENDIX

Appendix 1 – Component information

Table 12. Non-exhaustive list of components with their nomenclature and product reference

Circuit	Component description	Nomenclature (according to original hydraulic principle scheme)	Product reference
Heat pumps	Heat pump 1	VMP1	CRHV-P600YA-HPB
	Heat pump 2	VMP2	
	Heat pump 3	VMP3	
Source side towards heat pumps	Circulation pump	KB00-P01	LNES 50-160/55/P25VSC4
Source side towards ventilation	Circulation pump	KB1-P01	LNES 50-200/75/P25VSC4
Ventilation	Air handling unit 1	LB01	IV Produkt Envistar Flex 600
	Air handling unit 2	LB02	IV Produkt Envistar Flex 480
	Air handling unit 3	LB03	IV Produkt Envistar Flex 480
	Air handling unit 4	LB04	IV Produkt Envistar Flex 600
Sink side space heating	Circulation pump 1	VS00-P01	XLplus 65-120 F
	Circulation pump 2	VS1-P01	XLplus 80-120 F
Sink side DHW	Circulation pump 1	VS02-P01	XLplus 40-120 F
	Circulation pump 2	VS02-P02	XLplus 65-150 F
	Circulation pump 3	VS03-P01	XLplus 25-80
	Circulation pump 4	VS03-P02	XLplus 32-80 F
	Re-circulation pump 5	VVC1-P01	XLplus B 32-80
Wastewater recovery	Re-circulation pump	S1-P1	
DHW heat exchangers	cold water HX	VV1-VVX1	SL140-BR30-60-TL-LIQUID
	circulation HX	VVC1-VVX1	SL70-BR28-40-TL-LIQUID

Table 13. Technical data sheet of the heat pump units in Forsknigen 2. From Mitsubishi Electric – Air Conditioning Systems – 3rd edition.

Model		CRHV-P600YA-HPB	
Power Source		3-phase 4-wire 380-400-415V 50Hz	
SCOP(TDesign60kW):EN14825	Heat source temp 0/-3, Hot water temp 30/35	4.33	
Average climate conditions	Heat source temp 0/-3, Hot water temp 47/55	2.86	
Capacity1 *1		kW	60.0
		kcal/h	51,600
		BTU/h	204,720
	Power input *2	kW	14.2
	Current input 380-400-415V	A	24.0 - 22.8 - 22.0
	COP (kW / kW)		4.23
	Hot water flow rate	m ³ /h	10.3
	Heat source flow rate	m ³ /h	14.7
Capacity2 *1		kW	45.0
		kcal/h	38,700
		BTU/h	153,540
	Power input *2	kW	10.2
	Current input 380-400-415V	A	17.2 - 16.4 - 15.8
	COP (kW / kW)		4.41
	Hot water flow rate	m ³ /h	7.7
	Heat source flow rate	m ³ /h	11.2
Seasonal space heating energy efficiency class for medium-temperature application		A++	
Seasonal space heating energy efficiency class for low-temperature application		A++	
Maximum current input		A	44
Heat source fluid type		ethylene glycol 35WT% (freezing point -18°C (-0.4°F))	
Water pressure drop	Hot water side *3	kPa	14
	Heat source side *3	kPa	38
Temp range	Hot water side	°C	outlet water 30~65 *6
		°F	outlet water 86~149 *6
	Heat source side *4	°C	(inlet) less than 45, (outlet) -827
		°F	(inlet) less than 104, (outlet) 17.680.6
Circulating water volume range	Hot water side	m ³ /h	3.2 - 15.0
	Heat source side	m ³ /h	4.5 - 16.0
Sound pressure level (measured in anechoic room) at 1m *3		dB (A)	50
Sound power level (measured in anechoic room) *3		dB (A)	66
Installation location*5		Indoor use only	
Diameter of water pipe (hot water side)	Inlet	mm (in.)	50.8 (R2") screw
	Outlet	mm (in.)	50.8 (R2") screw
Diameter of water pipe (heat source side)	Inlet	mm (in.)	50.8 (R2") screw
	Outlet	mm (in.)	50.8 (R2") screw
External finish		Unpainted steel plate	
External dimension H × W × D		mm	1,561 × 934 × 780
Net weight		kg (lbs)	395 (871)
Design Pressure	R410A	MPa	4.15
	Water	MPa	1.0
Drawing	Wiring		KC94L652X01
	External		KC94L810X01
Heat exchanger	Hot water side		stainless steel plate and copper brazing
	Heat source side		stainless steel plate and copper brazing
Compressor	Type		Inverter scroll hermetic compressor
	Maker		MITSUBISHI ELECTRIC CORPORATION
	Starting method		Inverter
	Case heater	kW	0.035 × 2
	Lubricant		MEL32
Protection	High pressure protection		High pres.Sensor & High pres.Switch at 4.15MPa (601psi)
	Inverter circuit		Over-heat protection, Over current protection
	Compressor		Over-heat protection
Refrigerant	Type × original charge		R410A × 4.5(kg) × 2
	Control		LEV and HIC circuit

*1 Under Normal heating conditions at outlet hot water temp 95°F (35°C) outlet heat source temp 26.6°F (-3°C) inlet hot water temp 86°F (30°C) inlet heat source temp 32°F (0°C). Heating performance indicates the performance with counter flow of brine and refrigerant at the heat source HEX. (Standard pipe connection)

*2 Includes pump input based on EN14511.

*3 Under Normal heating conditions at outlet hot water temp 95°F (35°C) outlet heat source temp 26.6°F (-3°C) inlet hot water temp 86°F (30°C) inlet heat source temp 32°F (0°C) capacity 60kW hot water flow rate 10.3m³/h heat source flow rate 14.7m³/h. Heating performance indicates the performance with counter flow of brine and refrigerant at the heat source HEX. (Standard pipe connection)

*4 When using in inlet heat source temp is more than 27°C, please change to parallel piping at the heat source side.

* Please don't use the steel material for the water piping material.

* Please always make water circulate or pull out the circulation water completely when not using it.

* Please do not use groundwater and well water in direct.

* The water circuit must use the closed circuit.

* Due to continuing improvement, the above specifications may be subject to change without notice.

*5 Install the unit indoors only. Do not install outdoors.

